Zurich University
of Applied Sciences

School of Engineering

ICP Institute of Computational Physics

Research Report 2016

Zurich Universities of
Applied Sciences and Arts

www.zhaw.ch/engineering

Research & Development

OpenFoam based finite-volume simulation of conjugate heat transfer between a homogeneously heated spiral and an air steam. The air stream expands and doubles its Viscosity within $10\mathrm{cm}$.

OpenFoam basierte finite-Volumen Simulation der Wärmeübertragung eines homogen erhitzten Spiral-Heizelementes an einen Luftstrom. Der Luftstrom expandiert und verdoppelt die Viskosität innert $10\mathrm{cm}$.

Contents

Vorwort

Was treibt uns an? Wie motivieren wir uns für die Arbeit? Was steckt dahinter, wenn sich jemand besonders einsetzt? Gerade für die wissenschaftliche Arbeit, über die wir im vorliegenden ICP Forschungsbericht hauptsächlich berichten, beschreibt das schweizerdeutsche Wort Gwunder eine wichtige Antriebskraft. Im Gegensatz zur Neugier stammt unser Dialektwort von Wunder ab. Es betont die Leichtigkeit des Entdeckens und setzt den Forschenden in eine angemessene Demut. Natürlich sieht man in den hier präsentierten Zusammenfassungen als weitere Antriebskraft auch das Bestreben, etwas Nützliches zu schaffen. Dieser Ingenieursansatz wird durch den Gwunder angenehm angereichert und gestärkt.

In meinem ersten Jahr an der School of Engineering habe ich einen grossen Teil meiner Zeit damit verbraucht, die administrativen Abläufe zu verstehen und gute Lösungen für die effiziente Zusammenarbeit zu finden. Hier ist der Gwunder ein guter Ratgeber: Neben expliziten Regeln entdeckt man dabei auch eine informelle Ordnung; man findet interessante Entscheidungswege und erkennt menschliche und soziale Grundprinzipien wieder. Manchmal habe ich gestaunt und manchmal gelacht, so beispielsweise als mir mit einem Augenzwinkern erklärt wurde, dass erst mit der Einführung von *dunkler Materie* die Buchhaltung schliesslich aufgehe. Für die zahlreichen Hilfestellungen – stets wohlwollend und nützlich, manche mit Augenzwinkern und einer Prise Humor – möchte ich mich bei dieser Gelegenheit herzlich bedanken.

In der Diskussion mit engagierten Dozenten habe ich gesehen, dass didaktische Fragestellungen ebenso mit Gwunder und Entdeckergeist angegangen werden: Was geht in den Köpfen meiner Studenten und Studentinnen vor? In welchen Momenten wecke ich ihre Aufmerksamkeit? Was bleibt ihnen längerfristig von meiner Vorlesung in Erinnerung? Dank eines von der Internationalen Bodenseehochschule IBH geförderten Projekts dürfen wir uns etwas vertiefter mit der Didaktik befassen, was in Kapitel 5 genauer ausgeführt wird. Dies entspricht einer kleinen Neuerung in unserem bewährten Forschungsbericht: Wir möchten an dieser Stelle jeweils ein fürs ICP strategisch wichtiges Thema herauspicken und damit auch in die Zukunft schauen.

Es bleibt mir der Dank an alle Mitwirkenden und die Hoffnung, dass Sie als Leser jetzt gwundrig weiterblättern.

Andreas Witzig, Institutsleiter ICP, April 2017

1 Multiphysics Modeling

Multiphysics modeling is a powerful tool for exploring a wide range of phenomena, coupling flow, structure, electro-magnetic, thermodynamic, chemical and/or acoustic effects. The past decades have been a period of rapid progress in this area. In fact, a Google search of this neologism returns more than 600'000 results. The possible range of applications has been widely expanded and numerical methods have become increasingly sophisticated and adapted to exploit available computational resources. Today, detailed physical-chemical models combined with robust numerical solution methods are almost a necessity for the design and optimization of multifunctional technical devices and processes.
At ICP we perform applied research in the field of multiphysics modeling and develop finite element, as well as finite volume simulation software.
Our extensive experience in numerical analysis, modeling and simulation covers nearly all types of micro-macro devices and a wide range of governing equations of classical physics. We also develop single-purpose numerical tools specifically tailored to the needs of our partners, or use commercial software if better suited.
Among our specialities in this context is the application, extension and development of coupled models within our FE-inhouse code SESES, the CFD open source software openFoam and/or commercial products such as COMSOL Multiphysics.

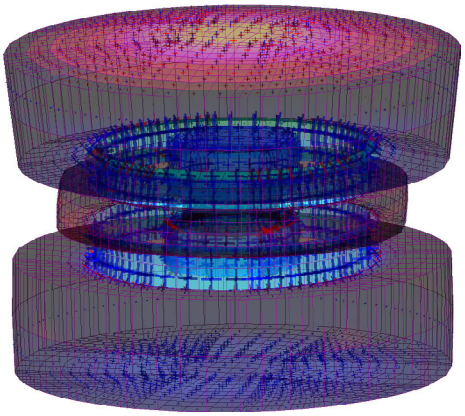

1.1 Numerical model of human skin

The ICP-spin-off Dermolockin GmbH developed a new diagnostic tool for skin cancer detection with active thermal imaging technology. In order to learn how to interpret the measurement data, the ICP developed a thermo-fluid dynamic model of the transient heat distribution within perfused human skin. Based on a sensitivity analysis of the thermo-physical properties of human skin, we determined, that the skin layer thicknesses and the blood perfusion rates are the most important parameters for the thermal response of the skin surface.

Contributors: T. Ott, G. Boiger, M. Bonmarin
Partners: Dermolockin GmbH
Funding: CTI
Duration: 2016–2017

Active thermal imaging consists of measuring and imaging the thermal radiation emitted from thermally stimulated objects. This technology is used for examining different types of skin lesions. Therefore, the skin surface is subject to an external thermal stimulation and the thermal recovery is monitored. Due to the different thermal recovery of healthy skin and lesions, one can obtain valuable information on the nature of the skin-fraction [1].

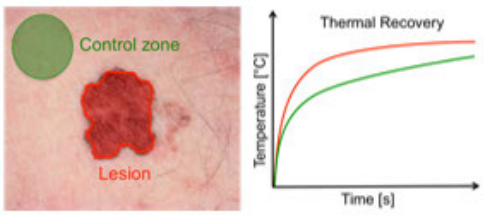

Fig. 1: Schematic of active thermal imaging measurement data of healthy skin (control zone) and lesion

The skin structure consists of five main layers, the stratum corneum, epidermis, papillary dermis, reticular dermis, and the hypodermis, where the latter three are perfused.

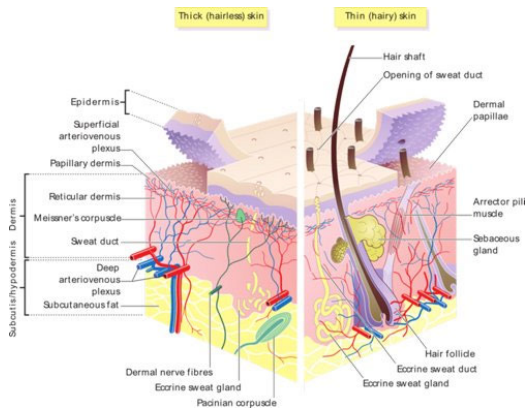

Fig. 2: Schematic representation of the human skin structure [2].

So far, the model only represents healthy skin. It takes into account heat transfer processes between the skin layers, perfusion within the skin layers, radiation, evaporation and convection between air and the skin surface as well as the thermo-physical property parameters of the skin.

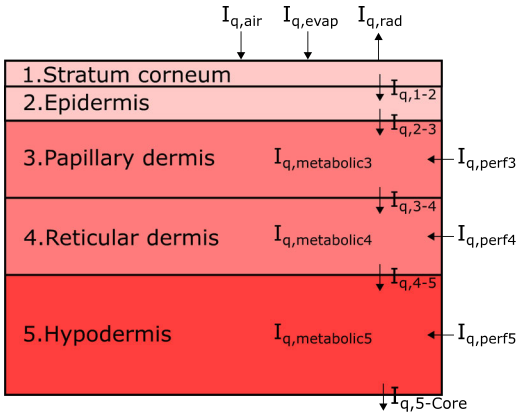

Fig. 3: Schematic of the skin model

In order to find out which parameters exert an important role on the skin surface temperature during thermal stimulation, a sensitivity analysis of the thermo-physical properties of the human skin was performed as in [3]. Therefore, we varied each parameter within a meaningful range and studied the respective impact on skin surface temperature. The analysis showed, that the skin layer thicknesses and the perfusion rates are the most important parameters with the strongest influences on surface temperatures.

Literature:

[1]: M. Bonmarin, F. Le Gal, *Lock-in thermal imaging for the early-stage detection of cutaneous melanoma: A feasibility study*, Computers in biology and Medicine, 2014.
[2]: M. Çetingül, C. Herman, *A heat transfer model of skin tissue for the dectection of lesions: sensitivity analysis*, Physics in Medicine and Biology, 5933-5951, 2010.
[3]: http://ucvts.schoolwires.net.

1.2 Model-based improvement of electro-kinetics in electro-winning using OpenFOAM

Highly pure copper suitable for the electrical industry can only be obtained by electro-winning. To increase the productivity of an industrial-scale plant, the influence of an additionally induced flow is studied. In order to do this, a model is developed which considers electro-kinetics and fluid mechanics.

Contributors: D. Brunner, G. Boiger

Partners:
Funding: ICP
Duration: 2016–2017

Electro-winning is a well-established industrial process, where lattice impurities are deposited during the process. In such plants the rate of the electrochemical reaction is limited by the natural convection which, along with electro-static diffusion, is the dominating effect of the ionic transport. Natural convection is a result of spatial variations in copper concentration inducing density gradients within the domain. These are accounted for by the Boussinesq approximation.

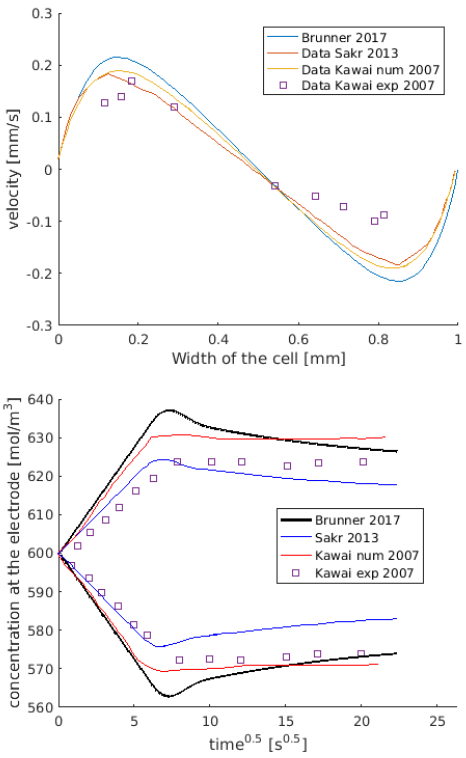

Fig. 1: Spatially dependent vertical velocity (top) and boundary concentration (bottom) at mid-height of 0.6 M CuSO4 B=1mm, H=10mm, J=20A/m², t=50s.

To test the accuracy of the code a validation was performed on a case originally conducted by Kawai et al. 2009 [1] and validated by Sakr et al. 2013 [2]. Thereby the vertical velocity profile and concentration at mid-height between two vertical electrodes was evaluated. The results are shown in Fig. 1. To increase the ionic transport of the cell, an additional flow was introduced at the lower end of the cathode.

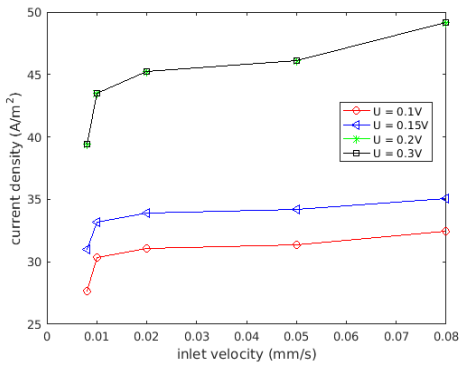

Fig. 2: Overall performance of the electro-chemical cells for different inlet velocities and applied potentials.

The performance of the cell can be determined by solving the electrochemical reaction and the induced electrostatic field. Kinetic effects are modeled by the Botler-Volmer equation and consider both electric potential and local concentrations. The additionally imposed flow increases the existing natural convection and decreases stratification within the cell. The higher ionic transport leads to a higher boundary concentration at the cathode where the reaction is limited. Both effects yield an increase of the overall performance of the electrochemical cell as shown in Fig. 2.

Literature:

[1] S. Kawai, Y. Fukunaka, S. Kida, *Numerical simulation of transient natural convection induced by electrochemical reactions confined between vertical plane Cu electrodes*, Electrochimica Acta, 52, 2007.

[2] I. Sakr, W. El-Askary, A. Balabel, K. Ibrahim, *Numerical Study on Natural and Forced Convection in Electrochemical Cells*, CFD Letters, 2013.

1.3 Gasifying Eucalyptus in Portugal

Due to its high cellulose-based water content, Eucalyptus has been known as a *hard-to-gasify* type of wood. Thus a prototype gasifier at the Aberta Nova site in Melides, Portugal, would just not run on this locally predominant wood species. In order to help out, a team of ICP researchers went to Portugal for several weeks, thoroughly analyzed the gasifier's process scheme and came up with a solution. The team modified the process such that the device now runs stable on any type of local wood.

Contributors: G. Boiger, T. Ott, C. Ritschard, P. Caels, G. Reinhard
Partners: Aberta-Nova-Stiftung
Funding: Aberta-Nova-Stiftung
Duration: 2016–2017

Wood gasification is a potential core-technology in the context of sustainable, de-centralized heat and electricity supply for homeowners as well as small and medium businesses. For years the ICP has conducted research in this field. Aside from extensive, model-based analysis of the process, we have constructed an experimental wood-gasifier in Thalwil. Our research partner, the Aberta Nova foundation, has constructed a prototype 20 kWel gasifier at their site in Melides, Portugal. While the aggregate runs quite smoothly on Pine, Eucalyptus causes problems concerning long-term stationary operation. Thus a team of ICP researchers was sent to Melides to analyze and amend the problem.

Fig. 1: T. Ott and C. Ritschard adapting the gasification device on-site at Melides, Portugal.

During the summer and autumn months of 2016, the ICP *gasification team*, composed of T. Ott, C. Ritschard and G. Boiger stayed at the Aberta Nova site for several weeks. Within this project they covered a wide spectrum of activities, involving planning, coordinating, analyzing, re-design, material acquisition and actual construction of an adapted gasification process. Thus they conducted a range of tasks, which clearly go beyond the traditional *modeling focus* of many other ICP projects. Fig. 1 shows T. Ott and C. Ritschard working at the generator (left), the reactor unit (middle) and the newly designed, external heat exchanger (right).

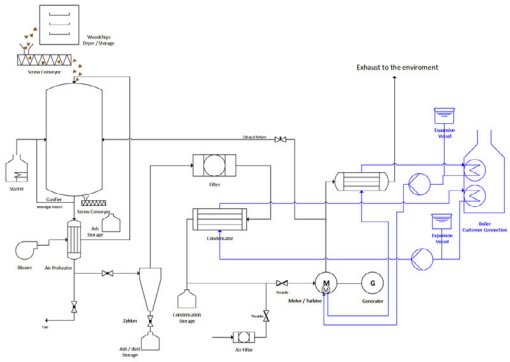

Fig. 2: Newly developed process scheme for more robust gasification process.

In very close cooperation with the Portuguese gasification-development team, lead by P. Caels and G. Reinhard, the ICP researchers were able to achieve a series of relevant results: (i) The existing gasification plant was analyzed such that a complete process scheme, along with full mass and energy balances could be elaborated. (ii) High wood-gas pressure drop, mainly caused by a condenser device, was identified as the main problem, which lead to preliminary ignition of the wood-gas mixture. (iii) As seen in Fig. 2, an adapted process scheme without the main condenser device was designed. (iv) All proposed changes, including the construction of a new, external heat exchanger were implemented directly at the plant. (v) Successful test runs, showing stable gasifier operation with Eucalyptus were conducted.

Literature:

[1] G. Boiger, *A thermo fluid dynamic model of wood particle gasification and combustion processes*, Int. J. Multiphys., 8 (2), 203–230, 2014.

1.4 Simulation von Heizelementen für Heissluftgebläse

Ein OpenFOAM-basiertes Simulationsmodell für industrielle Heissluft-Heizelemente wurde weiterentwickelt und alle relevanten Phänomene implementiert. Es umfasst nun Strömungsberechnungen, Wärmeübergänge, temperaturabhängige Materialwerte, sowie Strahlung in Fluid- und Solid-Regionen. Auf Basis der Simulationen wurden neue geometrische Konzepte mit dem Industriepartner Leister und den Forschungspartnern des IMPE entwickelt.

Contributors: M. Boldrini, G. Boiger, Th. Hocker

Partners: D. Penner group (ZHAW-IMPE), Leister AG
Funding: KTI
Duration: 2015–2017

Bei der Entwicklung neuer, optimierter Heizelemente für Heissluftgebläse ist es ausschlaggebend, dass die zugrundeliegenden physikalischen Vorgänge genau analysiert werden. Hierfür wurde bereits 2015 ein 3D-OpenFOAM-Solver entwickelt. Zur Erweiterung dieses *Conjugate-Heat-Transfer*-Solvers wurden verschiedene Strahlungsmodelle implementiert und verglichen. Letztlich wurde das Strahlungsmodell *viewFactor* gewählt, da dieses reale Effekte am besten abbildet. Weiter mussten zur Implementierung der Strahlung die Aussenwände des Strömungskanals als separate Wärmebilanzregion mitberücksichtigt werden. Es wurde erkannt, dass die Aussenwand einen entscheidenden Einfluss hat, da diese sich durch die Strahlung stark erwärmt und somit die Temperatur der Oberfläche, welche Energie an das Fluid überträgt, steigt (Abb. 1). Die gewählte Mesh-Geometrie soll die reale Geometrie eines einzelnen Heizkanals repräsentieren.

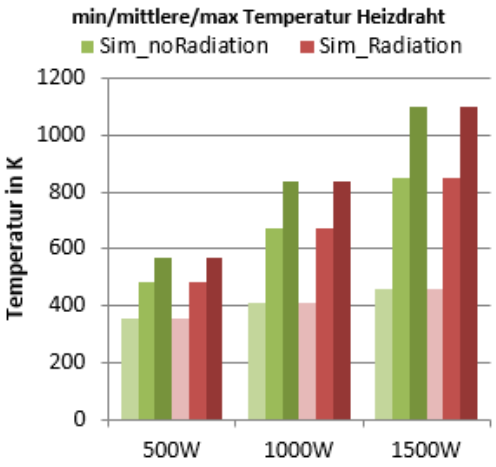

Fig. 1: Minimale, mittlere und maximale Temperaturen der Heizspirale und der Einfluss der Strahlung auf diese.

Auf Grund der Ergebnisse der Simulationen konnten die kritischen Bereiche identifiziert und aufbauend darauf neue geometrische Konzepte erarbeitet werden. Abb. 2 zeigt ein Beispiel, bei welchem es sich um eine extrudierbare Heizspirale mit zwei Kanälen handelt.

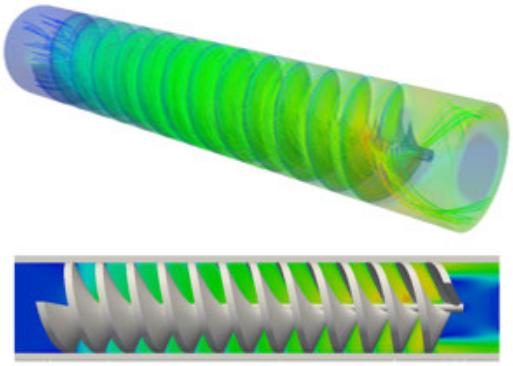

Fig. 2: Neues Geometriekonzept. extrudierbare Spirale als Heizelement und Strömungskanal

Durch die Windungen wird eine grosse Oberfläche über eine kurze Länge erzeugt. Simulationen zeigten, dass das Konzept grundsätzlich funktioniert und dass das Fluid, bei vertretbaren Temperaturen des Heizelementes, ausreichend aufgeheizt wird. Weiter wurde erkannt, dass durch die Drallströmung am Outlet eine homogenere Temperaturverteilung entsteht. Zur weiteren Verbesserung der Leistung wird nun eine Spirale mit nur einem Kanal entwickelt. Hierdurch soll der Stromfluss homogener werden und somit thermische Energie einheitlicher freisetzen.

1.5 Simulation des Nano-Dosier- und Ausströmverhaltens von nicht-Newtonschen Flüssigkeiten

Aufbauend auf früheren OpenFOAM-Modellen zur Ermittlung des Dosierverhaltens pharmazeutischer Fluide wurden sowohl weitere nicht-Newtonsche Fluide simuliert, als auch neue Modelle zur Vorhersage des Auftreff- und Ausströmverhaltens entwickelt. Simulationen des Ausströmverhaltens erzielten qualitativ akkurate Vorhersagen und quantitative Rechnungen wiesen Abweichung < 5 % zu den Messwerten des Industriepartners auf.

Contributors: M. Boldrini, G. Boiger

Partners: Novartis Pharma AG
Funding: Novartis Pharma AG
Duration: 2013–2016

Ein Modell zur Vorhersage von Dosiermengen hochfrequent injizierter pharmazeutischer Fluide wurde weiterentwickelt und die Bestimmung der Viskositätsfunktion verfeinert [1]. Aufgrund der systematischen Abweichungen von Wasser wurde ein für alle Fluide angewandter, konstanter Korrekturfaktor von 1.115 eingeführt. Mit diesem Modell und dem auf die Fluide angewandten Korrekturfaktor konnte sowohl für nicht-Newtonsche als auch für Newtonsche Fluide die dosierte Menge mit einer Genauigkeit von +/- 5 % für 90 % der Messpunkte bestimmt werden (Abb. 1).

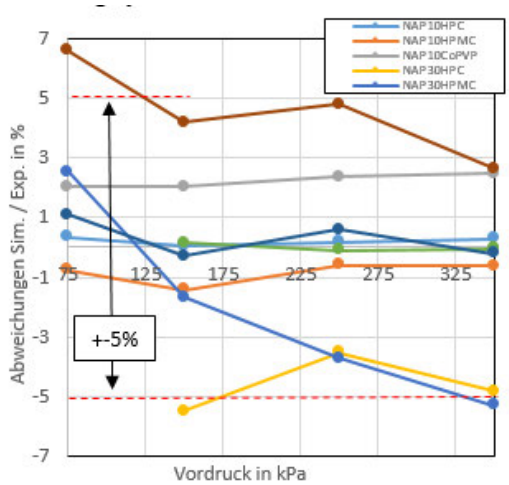

Fig. 1: Abweichungen der simulierten Dosiermengen im Vergleich zu Experimentalergebnissen.

Ausgehend vom Viskositätsmodell zur Bestimmung der Dosiermenge wurden zwei weitere Modelle für die qualitative Vorhersage des Dosiervorgangs verwendet. Die zweiphasigen Modelle basieren auf dem in OpenFOAM integrierten *interFoam-Solver*. Für die Berechnung des Abtropfverhaltens wurde eine 2-dimensionale Geometrie erstellt, welche als Simulationsbereich die gesamte Höhe von 20 mm vom Nadelaustritt bis zur Auftreffläche abdeckt. Für Newtonsche und leicht nicht-Newtonsche Fluide konnten sehr gute Übereinstimmungen bezüglich Vorhersage des Ausströmverhaltens erzielt werden. Bei sehr stark nicht-Newtonschen Fluiden, wie NAP30HPC, wurden die Abweichungen grösser, was auf die Definition und Messung der Fluideigenschaften zurückzuführen ist. Für die Vorhersage des Auftreffverhaltens wurde ein weiteres Modell entwickelt, welches sich nur auf den Bereich der Auftreffläche konzentriert. Hierfür wurde ein sehr fein aufgelöstes (9 Millionen Zellen) 3-dimensionales, ¼ Mesh erstellt.

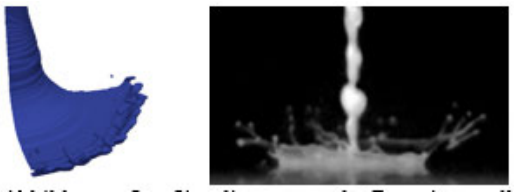

Fig. 2: Simuliertes und experimentell ermitteltes Auftreffverhalten.

Es konnte gezeigt werden, dass die Vorhersage des Auftreffverhaltens grundsätzlich möglich ist (Abb. 2), jedoch die Anforderungen an die Rechenleistung dabei beträchtlich sind.

Literatur:

[1] B. Bonhoeffer, M. Boldrini, *Experimental Characterization and Simulation of a Piezo-Actuated Micro Dispensing Valve*, J. Fluids Eng., 2016.

1.6 Modeling of electrostatic powder spray coating

Electrostatic powder spray coating is a widely used method to improve surface properties, by adding a protective layer onto the functional surface of a bulk material. The process involves various phenomena from aerodynamics, electrostatics and particle dynamics. An effective transient numerical OpenFOAM solver based on the finite volume method approach was developed and validated. Design concept enhancements and key process factors have been proposed and evaluated according to simulation results.

Contributors: S. Weilenmann, G. Boiger, B. Rutz, N. Reinke

Partners: Wagner International AG
Funding: CTI
Duration: 2014–2019

The simulations build up on an experimentally validated solver for the spray pistole (I) simulation [1]. Therefore a reduced coating chamber with four different powder spray pistols and an Al-plate, as shown in Fig.1, were initialized under common operating conditions.

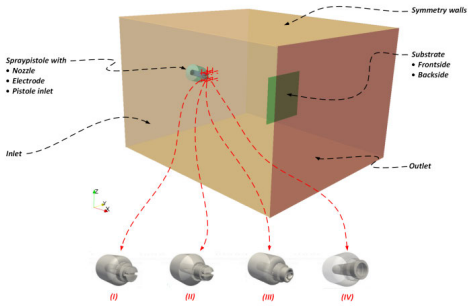

Fig. 1 Coating chamber model with boundary patches and nozzle design concepts The four nozzle concepts (I) fan nozzle , (II) opt. fan nozzle, (III) elliptical nozzle and (IV) tornado nozzle are shown from left to right respectively. The substrate is a square metal plate.

The ideas behind the design concept (III) are to divide the particle spray according to its destination (back or front) and to condense the spray cloud by using an elliptical shape. For the design concept (IV) a rotating injection duct and nozzle were proposed. Through centrifugal forces the different particle sizes get reorganized. The injection duct diameter shrinks with proceeding length up to the circular nozzle opening, where the shape expands to produce a cone cloud. For rising voltages, a decay in partial coating volume difference (PCVD) towards the ideal and an increase in transfer efficiency is visible, whereby the nozzle shapes (II) and (IV) have a similar enhancing effect. On the other hand, nozzle (III) yields, compared to the reference concepts (I, II), a poorer front-to-back particle division.

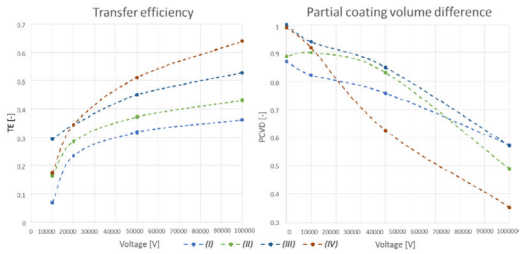

Fig. 2 Transfer efficiency and partial coating volume difference of (I–IV) depending on the applied voltage

A rise in the coating volume, particle-surface covering and reduction of rel. standard volume deviation under amplification of the applied voltage can be observed for the front and back sides. The rotating injection duct with a circular nozzle opening as in design concept (IV) seems to improve the efficiency, reduces PCVD and the relative standard volume deviation (RSVD) on the front side. On the other hand only larger particles adhere on the back side and hence amplification of the window frame is inevitable. The division according to destination of nozzle (III) is not yet effectively adjusted. The coating thickness on the front side is almost as high as for nozzle (IV), but on the back side the coating thickness of nozzle (III) is slightly improved compared to nozzles (I, II) and lower than nozzle (IV). Interestingly the RSVDs on the back side were reduced only with nozzle (III). To achieve better results, a 2D geometry optimization algorithm could be applied to optimally adjust the nozzles. So far design concepts have been proposed which could increase the efficiency and quality of the powder spray coating process.

Literature:

[1] G. Boiger, *Euler-Lagrangian Model of Particle Motion and Deposition Effects in Electro-Static Fields based on OpenFOAM*, Int. J. Multiphys., 10 (2), 2016.

1.7 Towards understanding the photovoltage in Cu_2O photocathode for hydrogen evolution

Electrolysis of water using solar energy in a single device frequently needs a suitable photocathode. In this work, we focused to understand the mechanism leading to photovoltage improvement and derived theoretical guidelines for best Cu_2O photocathodes.

Contributors: P. Cendula, M. Mayer

Partners: EPFL-LPI
Funding: SNSF
Duration: 2015–2017

Since the first investigations of Cu_2O photocathode at LPI EPFL during the PECHouse project, its photovoltage was one of the limiting factors. Specifically, only until last year the layer configuration was TiO_2/AZO/Cu_2O with photovoltage 0.3-0.6 V. Photovoltage for hydrogen evolution is equal to the onset potential since the reaction happens at 0 V vs. RHE. Following the developments in Cu_2O photovoltaic devices, the replacement of AZO buffer layer with Ga_2O_3 has recently brought great experimental improvement of photovoltage to 1.1 V at LPI EPFL.

The assumptions of our drift-diffusion model are (1) no interface recombination, (2) band edge pinning at the electrolyte interface, (3) TiO_2 conducts electrons like metal near H_2 evolution reaction, (4) charge transfer from conduction band of AZO or Ga_2O_3 to electrolyte, (5) thermionic emission at internal interfaces.

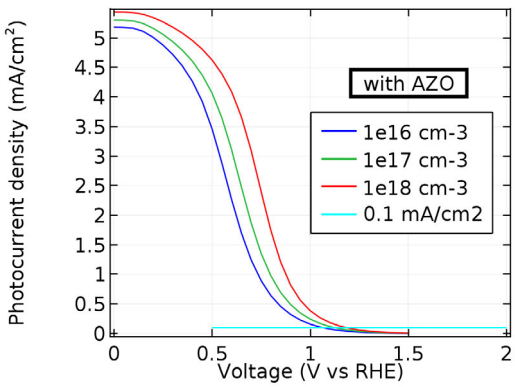

Fig. 1: Photocurrent-voltage curves with AZO buffer layer of varying doping concentration.

From the simulated IV, we extract photovoltage as the voltage where the photocurrent reaches 0.1 mA/cm^2. With the literature values of electron affinity for AZO (4.4 eV) and Ga_2O_3 (3.2 eV), and buffer layer doping 10^{16} cm^{-3}, the simulated values of photovoltage are 1.0 V vs RHE and 1.4 V vs RHE, respectively, see Figs. 1–2. The mechanism influencing the value of photovoltage is the formation of an energy barrier for electrons at one of the interfaces or speed of hydrogen evolution. The height of the energy barrier is influenced mostly by band alignments between individual semiconductors and their bandgaps.

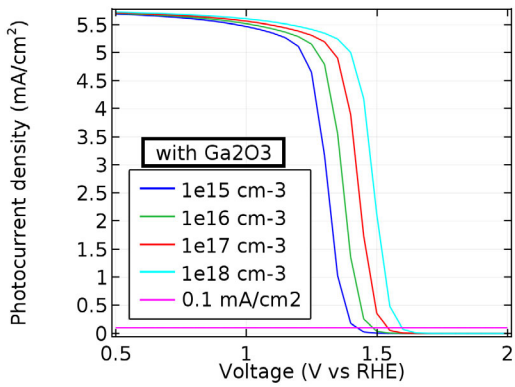

Fig. 2: Photocurrent-voltage curves with Ga_2O_3 buffer layer of varying doping concentration.

From the thermodynamic consideration of heterojunction energetics, we remark that photovoltage must be always lower than built-in voltage of the junction. One can also expect that increasing built-in voltage will increase photovoltage as well. From the analytical formula for built-in voltage $V_{bi} \sim \ln(N_D)$, we can thus expect that built-in voltage (and also photovoltage) will be larger for higher doping of the buffer layer, N_D. We observe this trend in our simulations results Fig. 1–2.

Based on the above equation we estimate a possible improvement of the photovoltage by 0.1–0.2 V by increasing the doping from 10^{16} to 10^{18} cm^{-3}. We note that other physical processes might be responsible for observed photovoltage as well, such as interface recombination, interface states and kinetic effects. Our work deems to use the simplest assumptions with a low number of free material parameters to qualitatively reproduce experimental behavior.

1.8 Scaled-up design of hydrogen generation from formic acid

The development of a chemical reactor converting formic acid (FA) to hydrogen for direct use with a polymer electrolyte fuel cell is very attractive for applications as decentralized power sources. Based on our validated numerical model of the reactor, we provide upscaling guidelines in order to reach 5 kW output capacity desired for first product prototype.

Contributors: V. Orava, O. Soucek, P. Cendula
Partners: EPFL, PSI, Charles University (CZ), Granit SA
Funding: Swisselectric Research, CCEM
Duration: 2014–2016

A multi-phase model of the gas and liquid flow, chemical reactions and heat transfer within the chemical reactor was written down in the first year of the project. We consider four phase transitions along the main chemical reaction (decarboxylation) - two evaporation mechanisms (FA, water) and two dissolved-gas-into-bubble diffusions (H_2, CO_2). We assume a general liquid mixture where the liquid solvent (FA and water) has one velocity field. In steady state the solvent forms an liquid-gas azeotrope with the constant ratio at 1 bar $\frac{\mathrm{FA}_{(l)}}{\mathrm{H_2O}_{(l)}} = \frac{\mathrm{FA}_{(g)}}{\mathrm{H_2O}_{(g)}} = 3$. Furthermore, the product of the decarboxylation is dissolved H_2 and CO_2 keeping the molar the ratio 1:1 and meeting the criteria of infinite dilution. The bubbles consist of ideal gaseous mixture of four gaseous constituents H_2, CO_2, FA, H_2O. The bubbles nucleate and grow (diffusion through the interface) due to the supersaturation of the liquid. In steady state, their overall rates keep the same ratio - the overall interfacial fluxes are constant. Our model was validated with measurements in the second year of the project.

To achieve desired power output of the reactor, the model predicts following scaling in power - Volume 1-50x, Temperature 120 ℃ - 4x, 130 ℃ – 7x, catalytic loading 10% - 1.75x, 15% - 2.3x, heating power 1-3x, heating surface/design 1-3x. We have set up scaled-up reactor model by enlarging the volume 5x, increasing the average temperature to 125 ℃, catalytic loading to 10.5% and heating power. The easiest replacement for the oil heating is electrical heating of wire. Since electrical wire delivers quite uniform temperature distribution contrary to heating by oil, we could easily produce high temperature at the top of the reactor if the long oil heating tube design would be used. Therefore, we suggest using electrical wiring only in the base of the reactor positioned slightly asymmetrically with respect to center in order to promote controlled circulation of fluid in the reactor. The simulation of the reactor showed desired electrical output of 5 kW, see Fig. 1. The temperature distribution shows hot-spots around the heating wires, which can be further eliminated by distributing heating power to multiple wires stacked vertically.

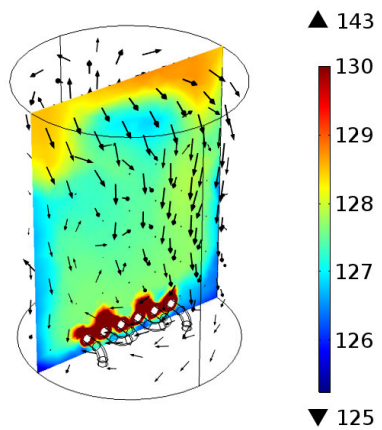

Fig. 1: Simulation on the scaled-up reactor with electrical wire heating, catalyst packing 10.5% vol. and reactor volume 3.4 litres (height 192 mm, radius 75 mm). Temperature distribution (in ℃) and velocity field are shown.

Depending on the measurements of next generation scaled-up reactor, future model investigations might focus on concurrent modeling of CO production, the role of bubble size on the reactor performance and floating of the catalyst particles. Although so far in the project formic acid was considered as a chemical commodity, significant research is done worldwide for large-scale synthesis of formic acid from atmospheric CO_2.

1.9 Thermisch-fluidisch-elektrisches FE-Modell hilft Temperaturen in einem elektrischen Schalter zu verringern

In elektrischen Bauteilen entstehen ohmsche Wärmeverluste, die zur Vermeidung von Temperaturspitzen gleichmässig an die Umgebung abgeführt werden müssen. Mithilfe eines FE-Modells wurden die Wärmestrompfade in einem elektrischen Schalter nachgebildet. Das Modell wurden anschliessend verwendet, um Anpassungen im Design zu machen, die eine gleichmässigere Verteilung der abzuführenden Wärme garantieren.

Contributors: T. Hocker
Partners: Unternehmen aus Elektrobranche
Funding: Direktfinanzierung
Duration: 2016

Wo viel Strom fliesst, entstehen in elektrischen Leitern sowie an deren Kontaktflächen unerwünschte ohmsche Wärmeerluste, die im Extremfall zu einer Überhitzung der Bauteile führen können. Diese thermischen Verluste können aufgrund von Alterungsprozessen – beispielsweise durch Oberflächenkorrosion – mit der Zeit sogar zunehmen. Einerseits besteht die Herausforderung darin, neue Produkte mit möglichst niedrigen ohmschen Verlusten zu entwickeln. Da sie sich jedoch nicht ganz vermeiden lassen, muss andererseits darauf geachtet werden, dass die entstehende Wärme möglichst gleichmässig an die Umgebung abgegeben wird.

Aufgabe dieses Projekts war es, einen elektrischen Schalter so umzugestalten, dass die darin auftretenden Maximaltemperaturen deutlich gesenkt werden. Hierfür wurde in enger Zusammenarbeit mit den Entwicklungsingenieuren des Auftraggebers ein thermisch-fluidisch-elektrisches FE-Modell in der ICP inhouse-software *SESES* entwickelt. Das Modell koppelt alle im Schalter auftretenden Wärmequellen aufgrund ohmscher Verluste mit den simulierten, lokalen elektrischen Stromdichten. Es berücksichtigt ausserdem den Wärmetransport aufgrund von Wärmeleitung, Naturkonvektion und thermischer Strahlung innerhalb des Schalters sowie vom Gehäuse an die Umgebung. Um die im Schalter auftretenden Temperaturen möglichst realistisch abzubilden, wurden die Anschlussleitungen sowie die Befestigungsschiene ebenfalls berücksichtigt. An allen elektrischen Kontakten treten ohm'sche Wärmeverluste sowie thermische Kontaktwiderstände auf, die die Temperaturen im Schalter stark beeinflussen. Thermische Kontaktwiderstände lassen sich nur unter sehr hohem Aufwand experimentell bestimmen. Deshalb wurden sie im Modell als Fitparameter behandelt und über lokale Temperatur- und Spannungsmessungen angepasst.

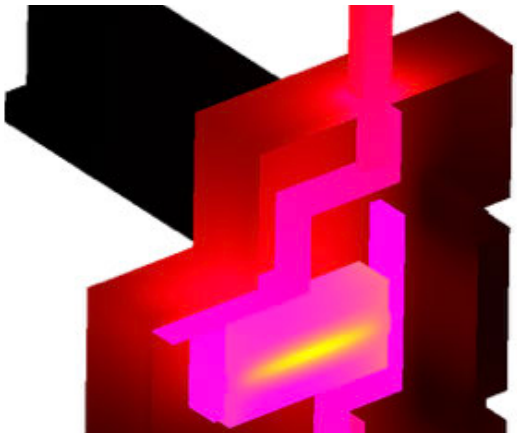

Fig. 3: Typische, vom *SESES* FE-Modell vorhergesagte Temperaturen im Inneren eines elektrischen Schalters.

Typische Temperaturen im Schalter sind in Fig. 3 dargestellt. Man sieht, dass die in Gelb dargestellten Maximaltemperaturen im Schmelzleiter der verwendeten Sicherung auftreten. Von dort fliesst ein Teil der Wärme an die stromführenden Bauteile und von dort über die Anschlussleitungen ab. Aufgrund des hohen elektrischen Stromflusses liegt die Temperatur der Anschlussleitungen selbst 1 m vom Schalter entfernt wegen der Eigenerwärmung der Leitung noch etwa 20 °C über der Umgebungstemperatur. Die verbleibende Wärme wird an das Gehäuse und von dort an die Umgebung abgegeben. Fig. 3 zeigt auch, dass die Wärmeabgabe vom Gehäuse an die Umgebung aufgrund der deutlich variierenden Gehäusetemperaturen nicht optimal ist.

Das kalibrierte FE-Modell wurden deshalb genutzt, den Effekt von Material- und Geometrieänderungen auf die Maximaltemperaturen im Schalter zu untersuchen. Aus den gewonnenen Erfahrungen konnten Designregeln abgeleitet werden, die schliesslich zu einem modifizierten Schalter mit deutlich verkleinerten Maximaltemperaturen führten.

1.10 Understanding anisotropic mechanical properties of shales at different length scales: In-situ micropillar compression combined with finite element calculations

Micropillars were compressed with an in situ scanning electron microscope (SEM) indenter with the aim to determine the micromechanical properties of the fine-grained porous clay matrix in Opalinus Clay. Thereby, vertical and horizontal stiffness as well as uniaxial anisotropic compression strength of the porous clay matrix were determined on the micrometer length scale. The determined values allowed an approximation of the transverse isotropic stiffness matrix related to the porous clay matrix, which can be used in combination with voxel based finite element modeling in order to gain insight into linear elastic behavior on mesoscale (millimeter-scale).

Contributors: L. Keller, J. Schwiedrzik, P. Gasser, J. Michler

Partners: EMPA, ScopeM
Funding: SHARC
Duration: 2016

From microstructural observations and experimental work it is known that shales consist of a mechanically weak porous fine-grained clay matrix with embedded and mechanically strong silt/sand grains. Thereby, the respective contents of weak and strong constituents control bulk mechanical properties. In addition, the clay matrix is characterized by a preferred orientation of clay platelets, which largely controls the bulk anisotropy of shales. To date little is known about the micromechanical properties of the fine-grained porous clay matrix, which is particularly true in case of its micromechanical anisotropy. Such information can, however, only be assessed on the microscale. Therefore, the drained micromechanical properties parallel and perpendicular to bedding were investigated by means of compressing micropillars with a flat punch indenter in a scanning electron microscope (SEM). Microscopic failure mechanism was found to be anisotropic: (i) in case loading was parallel to bedding it occurred by a combination of localized shearing, kinking/buckling of elongated clay aggregates and bedding parallel splitting, (ii) for loading perpendicular to bedding failure occurred mainly by localized shearing. The measured stiffness of the drained porous clay matrix perpendicular (Ev) and parallel (Eh) to bedding was about 8 GPa and 30 GPa, respectively. Using these stiffness values as input in voxel based finite element modeling and in combination with realistic microstructures, which are characterized with different contents of *soft* and *hard* constituents, revealed that the measured high microscale anisotropy Eh/Ev = 3.75 is crucial in understanding the bulk anisotropy of clay rocks.

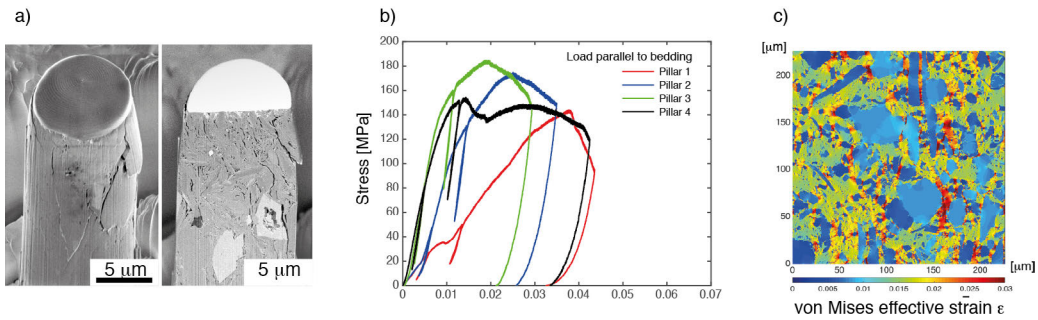

Fig. 1: (a) Micropillar after failure in case the load was applied parallel to bedding. Left is a SE image showing the whole pillar. Right is a BSE image showing a cross-section through the pillar. Orientation of the bedding plane is vertical. Note: (i) that the clay platelets tend to be vertical oriented and (ii) that failure is associated with the formation of multiple zones of localized shear deformation, kinking and axial splitting fractures. (b) Compressive stress-strain curves of micropillars for load parallel to bedding. The experimentally determined Young's moduli were used in combination voxel based FE simulations (Input = Image data). This allowed: (c) constructing von Mises effective strain maps, which show the distribution of strain in case an external strain is applied to a real clay rock microstructure.

1.11 Simulation of large-area semiconductor devices

Large-area thin-film semiconductor devices, such as solar cells or modules, suffer from electrical losses due to the sheet resistance in the various layers. These losses can be quantified depending on material and geometry parameters with the new Laoss simulation software by Fluxim AG. The ICP evaluates numerical methods for use in this software.

Contributors: C. Kirsch, S. Altazin, R. Hiestand, T. Offermans,R. Ferrini, L. Penninck, B. Ruhstaller

Partners: CSEM, Fluxim AG
Funding: CTI
Duration: 2016–2018

In a large-area semiconductor device, such as a solar cell or module, the electric charge generated inside the device due to light absorption needs to be transported towards the electrodes in order to produce electric current. Such a device typically consists of thin films, which exhibit sheet resistance. Because this resistance is inversely proportional to the film thickness the electrical losses are more pronounced in thin-film devices, in which the maximum electric power increases sublinearly with the device area. This effect of the sheet resistance on the device performance can be quantified by numerical simulation – some results are presented in Fig. 1.

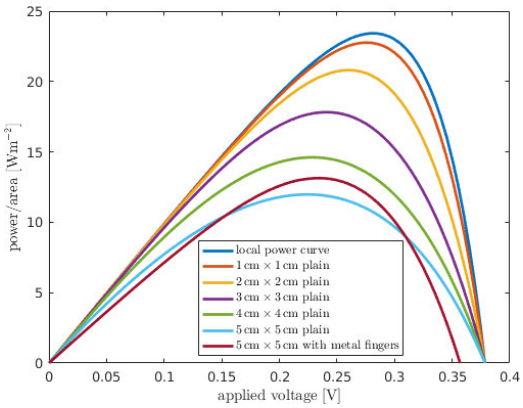

Fig. 1: Electric power divided by device area vs. applied voltage. Due to the sheet resistance, the maximum power increases sublinearly with the device area.

As a common solution to this problem metallic structures are applied to the electrodes – metal grid lines, for example, which are visible in most currently installed solar panels. While these metallic structures may improve the charge collection, they also cover a part of the electrode, such that light cannot enter the solar cell in these parts: There is a trade-off between enhanced charge transport and diminished light absorption.

The new Laoss simulation software by Fluxim AG assists the user in exploring this trade-off when evaluating different electrode designs for large-area devices. Laoss computes, for example, the electric output power depending on material properties and on geometry parameters. These parameters can be changed to assess their effect on the device performance. The simulation thereby helps to reduce the number of expensive trial-and-error stages during device fabrication. In the LAOSS CTI project, the ICP uses a prototype to evaluate some of the numerical methods for use in the Laoss software.

We employ a coupled 1D-2D modeling approach similar as in [1, 2] as well as the finite element method to simulate the charge generation and transport in the electrodes of a large-area semiconductor device. As an example, we illustrate the computed electric potential in the top electrode of a solar cell device with a metallic structure in Fig. 2.

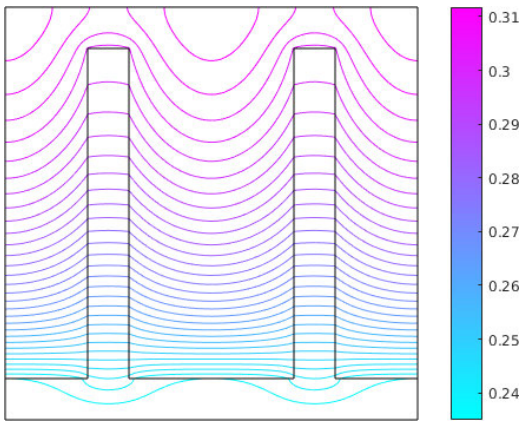

Fig. 2: Contour lines of the simulated electric potential $[\mathrm{V}]$ in the top electrode of a $5\,\mathrm{cm} \times 5\,\mathrm{cm}$ solar cell device with a metallic structure, at maximum electric output power. The electric current flow is orthogonal to these contour lines.

The maximum power computed for this device is larger than for the plain device with the same area, as shown by the two lowest curves in Fig. 1.

Literature:

[1] K. Neyts et al., J. Appl. Phys. 100, 114513, 2006.

[2] M. Slawinski et al., Org. Electron. 12, 1399–1405, 2011.

1.12 Computer simulations for producing delicious chocolate

The chocolate cooling process has a significant impact on taste and quality of the product. Nevertheless, the thermodynamic processes during this step are not well examined and understood. This knowledge-deficit led to a partnership between the ETH Zürich and the ICP. Together we use a combination of computer simulations and modern measurement methods to investigate the connection between mold geometry, cooling gas flow and heat transfer.

Contributors: D. Meier, T. Hocker
Partners: ETHZ, IFNH Food and Process Engineering Group
Funding: CTI
Duration: 2016–2017

A lack of control during the chocolate cooling process can lead to a loss of quality and to a energy consumption higher than necessary. the chocolate making process (HOTO) The chocolate cooling behavior is influenced by the thermal behavior of the product as well as the mold and cooling tunnel characteristics. Computer simulations are a useful instrument to improve the understanding of the mechanisms by which the heat released by the product is transferred to the surroundings. In addition, these models can be adapted for variable geometries and thus be used for mold and cooling tunnel optimizations.
Besides materials properties, heat transfer is strongly influence by the flow type of the cooling fluid.

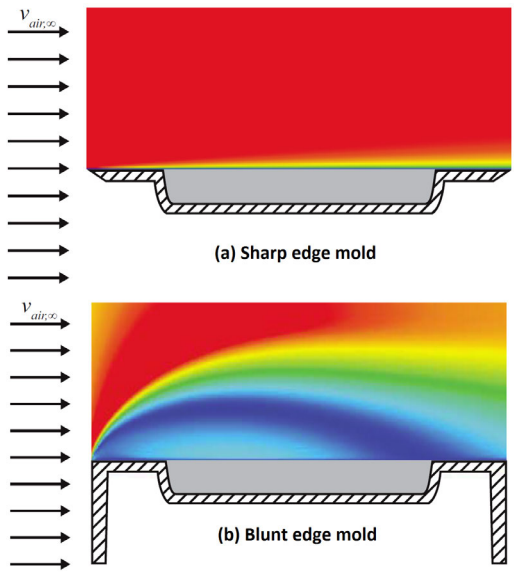

Fig. 1: Illustration of the two different mold types and the velocity distribution of the cooling air flowing above.

A fluid overflowing the mold and product surfaces ensures efficient, convective heat transfer. This is especially met with turbulent flows accompanied by vortices. We show in Fig. 1 how the flow behaviour of the cooling tunnel air can be influenced by the mold geometry. Though not apparent from Fig. 1, that higher turbulent energy production occurs with the blunt edge geometry. It turns out that the local heat transfer coefficient as shown in Fig. 2 correlates closely with the turbulent energy in the vicinity of the mold and chocolate surfaces. The maximum of the blunt edge local heat transfer coefficient (blue) lies at the location of the highest turbulent energy. This behaviour can be used to optimize local heat transfer in such complex geometries.

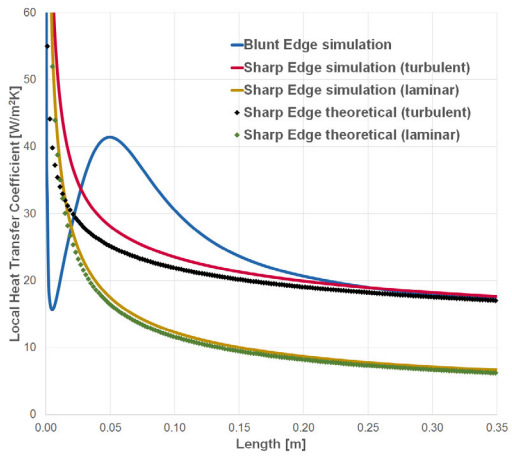

Fig. 2: Local heat transfer coefficient along the surfaces of sharp and blunt edge molds with cavities filled by some product.

Fig. 2 also illustrates the large difference between turbulent (red) and laminar (yellow) heat transfer. The comparison of these curves with Nu number correlations from the literature shows excellent agreement. Hence working with computer simulations allows target-aimed optimization of the mold and cooling channel geometries on a new level.

Literature:

[1] Rejmann, Lucie: Premium chocolate through cooling process optimization - and in-line monitoring approach, Diss. ETHZ 2017.

1.13 Parameter extraction from impedance spectroscopy of PEC electrodes

We work on the modeling of solar driven water splitting. One approach for construction of such a device is to use a semiconductor-based photoelectrochemical (PEC) cell. Extracting and comparing parameters of various PEC cells is the starting point for the improvement of their efficiency.

Contributors: P. Cendula, J. Schumacher
Partners: EPFL-LPI
Funding: Swiss Federal Office of Energy
Duration: 2015–2017

The rate of water oxidation at a semiconductor-electrolyte interface (denoted here k_{trh}) is usually a limiting factor for many photoelectrode materials. The quantification of the water oxidation rate is not direct in most of the literature sources, but a similar parameter called charge transfer resistance is extracted from an equivalent circuit (EC) of the electrical impedance spectroscopy (EIS) measurement. Although EIS provides means of probing the photoelectrode properties within a large range of characteristic frequencies, its interpretation is frequently cumbersome and limited to EC models which provide phenomenological parameters but not directly physical parameters of the system.

To overcome this bottleneck, we have derived a transient drift-diffusion model of EIS and used it to extract physical parameters. In EIS a small harmonic potential perturbation is applied to the PEC cell. We solve for a stationary solution first and then we assume that the transient solution can be linearized around the stationary solution. We arrive at a system of partial differential equations for the perturbed variables and solve them numerically in the frequency domain.

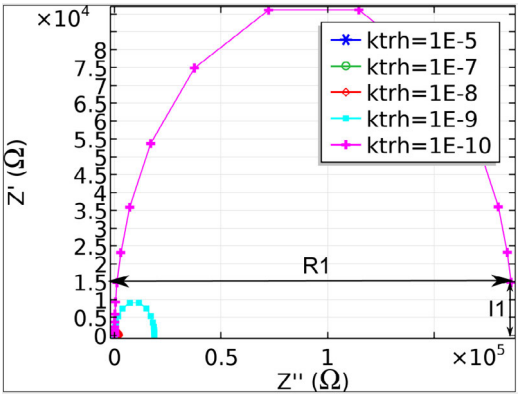

Fig. 1: Nyquist plot of impedance under illumination for various values of k_{trh} and a fixed potential of 0.7 V vs. RHE.

We have used material parameters of a hematite photoanode for our calculations. Under light illumination, transient simulations for a range of frequencies $10^{-3} - 10^{7}$ Hz is undertaken and presented in the form of a Nyquist plot, Fig. 1. The Nyquist plots exhibit a single semicircle, pointing to a capacitive behavior of the electrode. We investigated the dependence of the real (R_1) and imaginary (I_1) part of the lowest frequency impedance on the rate constant k_{trh}, for a potential of 0.7 V vs. RHE, slightly higher than the flatband potential, Fig. 2.

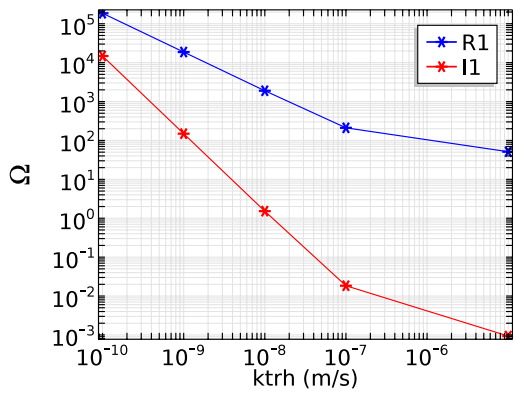

Fig. 2: Dependence of the lowest frequency (10^{-3} Hz) impedance for 0.7 V vs. RHE (left) on the rate of water oxidation k_{trh} for fixed $t_h = 48 \cdot 10^{-7}$ s.

The linear relation between R_1 and k_{trh} is obtained from simulations, Fig. 2. A similar relation was obtained between R_1 and the recombination rate t_h (not shown). Thus, governing processes for the semicircle size are both electron-hole recombination and the rate of water oxidation. Their values can be extracted from a comparison of measured and simulated impedance data.

Our model is applicable to many materials investigated for PEC water splitting.

1.14 Numerical modeling of SOFC electrodes

In this work, we are primarily interested in improving the performance of anode electrodes of high temperature solid-oxide-fuel-cells (SOFC) by means of numerical methods and by fitting electrochemical impedance spectroscopy data (EIS).

Contributors: G. Sartoris, L. Holzer
Partners: Hexis AG
Funding: SNSF
Duration: 2014–2017

At the beginning, the SOFC electrodes were made of two solid-phases, i.e. two different materials, building up a porous matrix, where each phase was transporting either electrons or ions. With this approach, the oxidation or reduction tooks place at the so called triple-phase boundary (TPB), a topological one-dimensional subspace at the conjunction between the two porous solid-phases and the pores of the gas phase. For example, for the reduction of oxygen $1/2\mathrm{O}_2 + 2e^- \rightarrow \mathrm{O}^{2-}$ at the cathode, one solid-phase was transporting the electrons $2e^-$ coming from the positive electrical contact, then at the TPB the oxygen $1/2\mathrm{O}_2$ delivered through the pores was reduced to O^{2-} and injected into the other solid-phase and further transported to the electrolyte just letting these oxygen ions to pass through.

A new and apparently better promising approach (here for the Hexis anode) consists in using a single mixed ionic electronic conducting (MIEC) solid phase transporting both electrons and ions with the advantage that oxidation or reduction now takes place at the topological two-dimensional surface between the solid material and the pores. Again as an example for the reduction of oxygen, electrons from the electric contact are injected and transported in the solid MIEC-phase towards the two-dimensional interface where they are consumed to reduce the oxygen delivered through the pores; now the reduced oxygen O^{2-} at the interface is injected in the solid MIEC-phase and further travels towards the electrolyte. The advantage of this approach is the larger area available for the reduction/oxidation and so one expects better performances i.e. less electrical losses. Cerium oxide CeO_2 (ceria) is a material of interest for the anodic MIEC phase. Within the crystal lattice, we have strong bond cations Ce^{4+} and weak bond anions O^{2-}, where these latter can diffuse and migrate through the lattice, however, at large oxygen partial pressure the electronic conductivity is low. In order to make this MIEC material an electronic conductor, one lowers the oxygen partial pressure so that anions O^{2-} are removed from the lattice leaving behind (positive charged) oxygen vacancies $\approx 10^{18} - 10^{19}\mathrm{cm}^{-3}$ and (with respect to Ce^{4+} negative charged) cations Ce^{3+} so that electrons can hop through Ce^{3+} (polaron-hopping).

In a first approach, we may model the SOFC consisting of a cathode and anode as described above. From a multiphysics point of view, we then have to compute the oxygen/hydrogen concentrations in the cathode/anode gas pores, the oxygen ion concentrations in the cathode/anode MIEC-phase, the oxygen ion concentrations in the electrolyte and the electric potential together with the electron concentration everywhere except in the gas pores. Since the lateral dimensions of the SOFC are much larger than the vertical one where the electric driven transport takes place, we actually do not have to compute the whole SOFC but we can limit ourselves to compute a vertical tube through the SOFC; eventually by applying periodic boundary conditions on the vertical facets.

The advantage of using a 3D numerical model is that we just need the values of some bulk parameters together with the ones of injection currents which are then fitted from EIS data. However, full 3D harmonic models are still computational prohibitive, so that with model reduction one tries to obtain a simplified but still valid model being able to reproduce EIS data.

1.15 A novel lighter-than-air wind power turbine

More than 1.16 billion people around the world are living in off-grid regions. Since 2012 our initiative aims to develop a new lighter-than-air wind power turbine to harvest the power of strong winds at high altitudes. The system is compact, cost-effective and eco-friendly to be used in remote off-grid locations. We are conducting research on the development of the rotor part of the system through numerical simulations, wind tunnel experiments and blade material tests. Valuable results show the power performance of the new rotor and the ability of the materials to withstand strong wind and weathering conditions.

Contributors: Y. Safa
Partners: IMPE, ZAV
Funding: Swiss Federal Office of Energy
Duration: 2016–2017

The technology of Airborne Wind Energy (AWE) aims to develop new systems that operate to harvest strong wind power at several hundred meters above ground level. At that altitude, wind currents are stronger and much more stable than those close to the ground. For the installation of the wind power system at that altitude, buoyant gas aerostat are deployed to carry an electrical generator which hovers in the sky with a cable-tether connection to the earth.

Since 2012, several development steps have been conducted on a new lighter-than-air wind power turbine. Several tests on the proof-of-concept have been performed with on-ground and in-sky open-field trials. The tests have successfully shown the operation of a novel rotor that exhibits an increased performance at reduced weight-to-swept-area ratio. Two patent applications have been submitted. A report of techno-economic analysis have been prepared, showing the promised potential of the new technology.

Moreover, a new proprietary bionic concept of the rotor has been developed. Beside being bird-friendly, the new rotor mimics the birds' interaction with the wind to produce both power-generating forces and elevation forces. Therefore, the tethered airborne system hovers in the strong winds with limited blowdown angle, using a reduced amount of buoyancy gas. This is due to the *self-lifting* aerodynamics of the new rotor's concept.

Currently, further research efforts supported by SFOE, the Swiss Federal Office of Energy, are aimed at the further development of the technology. A small-scale model combining numerical simulations, material tests, and wind tunnel experiments is applied to develop the new rotor.

Fig. 1: Energy coming from the sky is more than clean.

Investigations of the influence of geometry on the rotor performance are aimed at a new design and arrangement of the blades for improved power generation.
Three institutes from the School of Engineering (SoE) are contributing to this project. They are providing expertise in mechanical design and computational simulations at ICP, aerodynamic testing in wind tunnels at ZAV and light-weight polymer materials development and testing at IMPE. Valuable results are obtained that show the power performance of the new rotor and the capability of tested materials to ensure the aerodynamic service of the blade under wind loading and weathering conditions.
A symbol of our Airborne Wind Power initiative is depicted in Fig. 1. A spin-off company will be founded soon to provide communities in remote regions with environmentally friendly power sources.
ZARAWIND is thankful for the support mainly from T. Hocker, D. Wilhelm, A. Witzig, G. Boiger, C. Meier, C. Brändli, M. Guillaume, L. Manefriani and many others.

2 Fuel Cells and Microstructures

Fuel cells are a prime example of electrochemical cells. They convert fuels such as hydrogen, natural gas or methanol into electrical energy and heat. Fuel cells can be used as a battery replacement in portable electronic devices, for combined production of heat and electricity in households and as electricity source in vehicles. Due to their flat design, fuel cells are easily scalable by connecting them in series to form stacks. Electrical efficiencies over 60 % are feasible which is much higher compared to other decentralized electricity generation technologies. Although the working principle among all fuel cells is the same – i. e. they all are galvanic cells –, they greatly differ in the choice of used materials and feasible operating temperatures.
The ICP supports the progress in fuel cell research by developing multiphysics computer models. In general, modeling helps to better understand the large number of chemical, thermal, electrical, mechanical and fluidic processes with the goal to detect weaknesses of the system and provide design improvements. Often these models rely on detailed information about the microstructures of the investigated materials. Hence the characterization of e. g. electrode and electrolyte microstructures in 2D and 3D is an integral part of our modeling efforts. Since this is a very time-consuming method we started a collaboration with the group of V. Schmidt, Universität Ulm, to use stochastics to generate virtual microstructures with identical properties to real microstructures, see the example blow. This allows one to test and optimize the performance of microstructured materials in a much more efficient way.
In addition to fuel cells, we also do research on novel hydrogen production techniques. For example, we model photo-electro-chemical cells (PECs) which use solar energy to split water and thus produce hydrogen fuel.
Most research projects are conducted in collaboration with our strategic partners Hexis AG in Winterthur (SOFC), Paul Scherrer Institut in Villigen (PEFC), EPFL (hydrogen generation) in Lausanne and Universität Ulm (virtual microstructures).

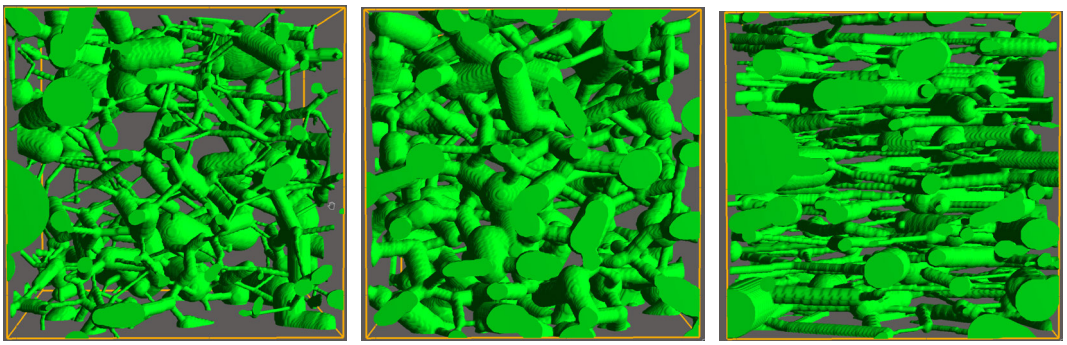

2.1 3D analysis of liquid water in gas diffusion layers of polymer electrolyte fuel cells

The performance of polymer electrolyte fuel cells (PEFC) strongly depends on a controlled water management in the porous layers. For this purpose we investigate liquid water transport in a commercial gas diffusion layer (SGL 25BA) by means of X-ray tomography and 3D image analysis. The study provides a quantitative understanding of micro-macro relationships in GDL.

Contributors: L. Holzer, O. Stenzel, O. Pecho, B. Münch, J. Schumacher, A. Lamibrac, F. Büchi

Partners: PSI, EMPA
Funding: SNSF
Duration: 2014–2017

X-ray tomography experiments combined with pressure-induced water injection were performed at PSI. These experiments provide 3D images of the liquid water distribution inside the GDL at incremental pressure steps between 0 and 100 mbar. The breakthrough behavior of the liquid phase is highly anisotropic. In through-plane (tp) direction the 'breakthrough' evolves continuously over an extended pressure range from 5 to 30 mbar. For in-plane (ip) direction the breakthrough is discontinuous and takes place at 27 mbar. 3D simulations of the intrusion process in thin GDL layers reveal that the different breakthrough behaviors are mainly triggered by different ip- and tp-transport distances. The observed anisotropy is thus attributed to a so-called short-range effect that controls the tp-breakthrough.

Dedicated methods for 3D-image analysis were developed to quantify the microstructure characteristics relevant for liquid permeability. Quantitative relationships are established between these microstructure characteristics and the liquid permeability, which provide a better understanding of the underlying microstructure limitations for injection and liquid transport.

The curves for relative permeability vs. saturation (and capillary pressure) achieved from 3D-analysis reveal complex but characteristic shapes with concave, linear and convex segments, see Fig. 1. The shape of these segments can be attributed to distinct microstructure effects. In contrast, the conventional macroscopic descriptions from literature cannot capture these complex shapes and the underlying microstructure effects. Future investigations with different GDL materials are necessary in order to understand whether these complex permeability-curves represent a general feature of GDL or if they are specific to the investigated SGL material.

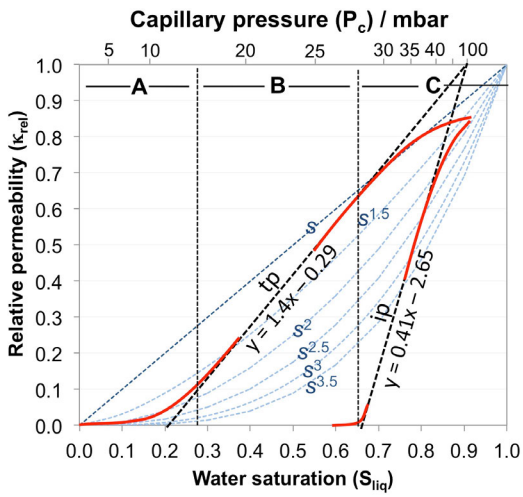

Fig. 1: Relative permeability curves for in-plane (ip) and through-plane (tp) directions in GDL obtained from injection experiments combined with X-ray tomography and 3D analysis.

Literature:

[1] L. Holzer et al., Electrochim. Acta, 227, 419–434, 2017.

2.2 Development of cost effective fuel cell systems

The Swiss Competence Center for Energy Research - Efficient Technologies and Systems for Mobility (SCCER Mobility [1]) - is a research program initiated in January 2014. The aim of the program is to find new mobility solutions and products with a measurable impact on energy efficiency and reduction in CO_2 emissions. One of the main focal points in the first three-year-stage was on the development of a novel concept of thermo-neutral fuel cell operation. The initial indications are very promising as the concept provides the cost reduction of the fuel cell system while maintaining or even slightly increasing the overall performance.

Contributors: J. Dujc, A. Forner-Cuenca, M. Cochet, P. Marmet, J. Schumacher, P. Boillat
Partners: PSI
Funding: CTI
Duration: 2014–2017

The essential feature of the thermo-neutral fuel cell concept is cooling of the fuel cell by means of water evaporation. Besides the positive effects of the presence of liquid water in a fuel cell, the cooling effect and the increased efficiency due to improved membrane conductivity, there is also the risk of reduced cell performance. Namely, the liquid water tends to block the pathways through the porous gas diffusion layer (GDL) and thus limits the transport of reactant gases.

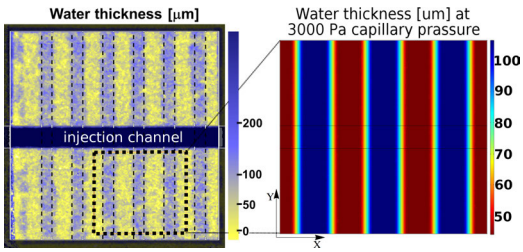

Fig. 1: The neutron imaging (left) and the numerically obtained (right) distribution of the total water thickness in the patterned GDL. A cell with 1×1 cm of active area was used in the experiment while a smaller portion was considered in the simulation. The water accumulates in the hydrophilic domains.

To avoid the potential risk and to exploit the evaporative cooling, our partner, the Paul Scherrer Institut, developed a new patterned GDL design [2]. The pattern consisting of hydrophobic and hydrophilic regions ensures the movement of liquid water into the predefined directions and establishes blockage free paths for reactant gases.
In the first stage of the SCCER the performance of the new material was tested in ex-situ and in-situ experimental conditions at PSI [2]. In parallel to the experimental work, the team at the ICP developed numerical models of the new material and of the operating fuel cell. Both the experiments and the models show that the water accumulates in the hydrophilic regions, see Fig. 1. The initial experimental data indicates that the performance of the operating cell is slightly improved when using the new GDLs. The numerical model of the operating fuel cell was used to study the intricate couplings in the thermo neutral concept, see Fig. 2 and [3].
The second stage of the SCCER Mobility started in January 2017. The short term goal for this stage is to demonstrate the proof of concept of the thermo-neutral systems operation while the long term goal is the development of the system prototype. The role of the ICP is to provide accurate numerical models that can be used as tools to optimize the system and its components towards higher efficiency, higher energy density and improved reliability.

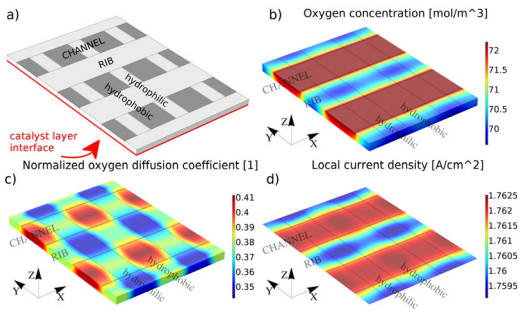

Fig. 2: a) the geometry of the FC model consisting of the rib and channel regions which are perpendicular to hydrophilic/hydrophobic pattern, b) the distribution of the oxygen concentration, c) the distribution of the saturation dependent oxygen diffusion coefficient and d) the local current density distribution. Both the rib/channel and the hydrophilic/hydrophobic pattern play a role in the distribution of liquid water, the distribution of gases and the final local current density. As expected we obtain the highest current under the channels in the hydrophobic region and the lowest current under the ribs in the hydrophilic regions, where the liquid water blocks part of the pore space.

Literature:

[1] http://www.sccer-mobility.ch/
[2] A. Forner-Cuenca et al., Advanced Materials, 27 (41), 6317–6322, 2015.
[3] J. Dujc et al., Journal of Electrochemical Energy Conversion and Storage, Submitted, 2016.

2.3 The importance of electrical contact resistance for predictive PEFC simulation

In computational models of polymer electrolyte fuel cells (PEFCs), interfacial resistances between the different contacting material layers are often disregarded. Various experimental conductivity measurements have shown, though, that they can have a significant share in the overall through-plane resistance. Recently, we have implemented experimentally measured contact resistances into a one-dimensional stationary two-phase PEFC model to examine their impact on cell performance prediction.

Contributors: R. Vetter, J. Schumacher

Partners: PSI
Funding: SNSF
Duration: 2014–2017

Contact resistance is a consequence of imperfect contact between rough surfaces. Thermal and electrical contact resistance between individual layers in a membrane-electrode assembly are known to have a large impact on cell performance and may even dominate over bulk resistance [1]. Interfacial resistance depends on the compressive load on the cell, which is applied to increase conductivity and to better seal the gas flow channels. Yet, it is often neglected in numerical modeling of PEFCs.

Scaling arguments for contacting fractal surfaces predict that the relationship between contact resistivity R and applied clamping pressure P obeys a power law $1/R \sim P^{\alpha}$ with exponent $\alpha \in [1/2, 1]$ depending on surface roughness and plasticity [2]. Published experimental measurements on typical PEFC materials such as Gore membranes, SGL and Toray carbon papers and stainless steel or graphite plates are indeed consistent with this prediction in the relevant pressure range [3]. As an example, the electrical contact resistivity between a gas diffusion layer and a bipolar plate from ref. [4] is plotted on a log-log scale in Fig. 1a.

To examine the importance of taking interfacial resistance into account, we implemented these power laws into a steady-state, non-isothermal, two-phase finite element PEFC model in COMSOL Multiphysics (Fig. 2). A selection of simulation results with and without contact resistance is shown in Fig. 1b for standard operating conditions (vapor-saturated hydrogen and air at 80°C and 2 bar) and different compressive loads. Our simulations demonstrate that electrical contact resistance is responsible for a significant voltage loss even at high clamping pressures and that this performance drop increases with current density. These results challenge researchers in PEFC modeling not to neglect interfacial resistance in their computational studies. Appreciating contact resistance constitutes an important step toward more predictive fuel cell simulations.

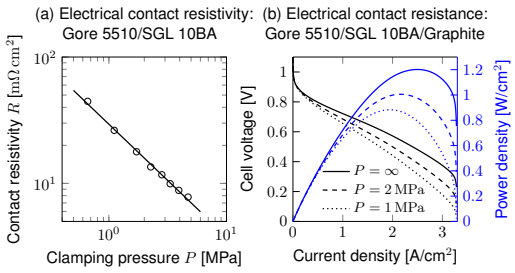

Fig. 1: (a) Experimental data of electrical contact resistivity as a function of clamping pressure. (b) Effect of contact resistance on fuel cell performance as computed with the 1D finite element COMSOL model.

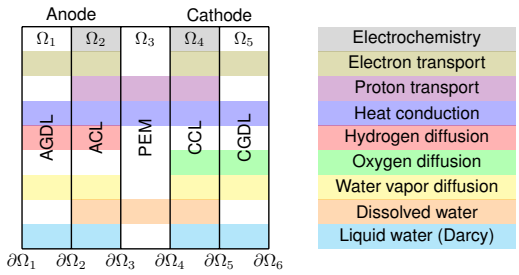

Fig. 2: Simplified sketch of the PEFC model (not to scale).

Literature:

[1] L. Cindrella et al.J. Power Sources, 194, 146–160, 2009.
[2] A. Majumdar, C. L. Tien. J. Heat Transfer, 113, 516–525, 1991.
[3] P. Zhou, C. W. Wu, G. J. Ma. J. Power Sources, 159, 1115–1122, 2006.
[4] I. Nitta, O. Himanen, M. Mikkola. Electrochem. Commun., 10, 47–51, 2008.

2.4 Interfacial water droplet formation model for PEFCs

Liquid water transport and phase change are crucial for efficient operation of polymer electrolyte fuel cells (PEFCs). In particular the interfacial mass transport condition between gas diffusion media and flow channels is poorly understood. Within this project we develop a combined water droplet formation, detachment and evaporation model to obtain more realistic flux boundary conditions for macro-homogeneous two-phase PEFC simulations.

Contributors: R. Vetter, P. Marmet, J. Schumacher

Partners: PSI
Funding: CTI
Duration: 2014–2020

The interface between the porous gas diffusion layer (GDL) and the gas channel (GC) is notoriously difficult to model realistically in PEFC simulations involving liquid water transport. Little droplets grow, evaporate and are transported away by the incident transverse gas stream. Inspired by an idealized view of single-capillary droplet growth [1], we have developed an analytical interfacial droplet formation model (Fig. 1).

Given the accumulated droplet volume and its corresponding radius R, the model predicts an interfacial pressure p via the Young-Laplace equation $p = 2\gamma \cos\theta / R$, where γ is the surface tension of water and θ its (averaged) contact angle on the GDL surface. An implementation in COMSOL Multiphysics (Fig. 2) shows good quantitative agreement between analytical model and simulation.

When drag forces in the gas stream eventually exceed the adhesion forces on the interface [2], the droplet is removed from the GDL surface and the process is repeated, leading to a periodically fluctuating interfacial pressure (Fig. 3). This pressure can then be averaged over a distribution of droplets and over time to derive a Neumann boundary condition for use in macro-homogeneous two-phase PEFC simulations, which is current work in progress. The model also allows to estimate the local amount of interfacial area available for water evaporation, thus enabling to formulate a combined liquid/vapor mass transfer rate at the interface.

X-ray tomography imaging of the process is currently being performed at the Paul Scherrer Institute to quantify the dynamics of water pullback within the GDL after droplet detachment and to verify the validity of the droplet concept.

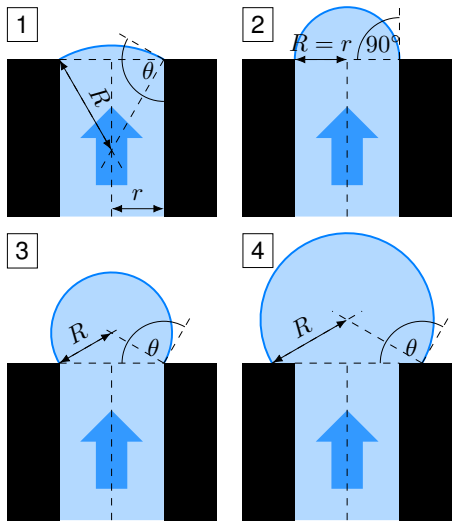

Fig. 1: Idealized water droplet formation before detachment at the GDL/GC interface (from 1 to 4).

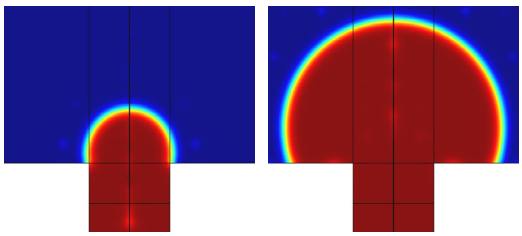

Fig. 2: Numerical simulation of water droplet formation in COMSOL Multiphysics (water in red, air in blue).

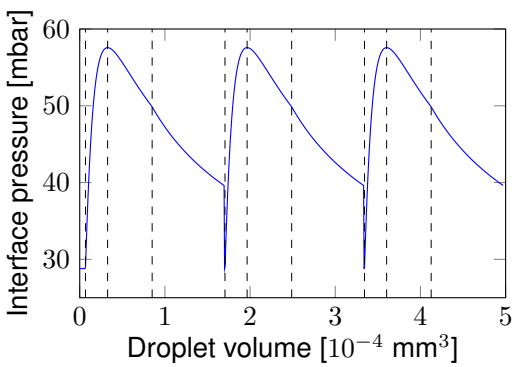

Fig. 3: Periodic evolution of interfacial capillary pressure as a result of droplet formation and removal.

Literature:

[1] R. Wu, Y.-M. Li, R. Chen, X. Zhu. Int. J. Heat Mass Transfer, 75, 668–684, 2014.

[2] F. Y. Zhang, X. G. Yang, C. Y. Wang. J. Electrochem. Soc., 153, A225–A232, 2006.

3 Organic Electronics

Organic semiconductors have received great attention since 1987 when organic light-emitting devices were invented by leading scientists at Kodak USA. After 30 years of R&D and commercialization efforts world-wide, we are now witnessing a wide range of OLED displays in consumer products ranging from mobile phones to 77 inch TVs. The particular advantages of OLEDs is their thin construction, large viewing angle, color gamut and high energy conversion efficiency. OLEDs consist of a sequence of thin organic semiconductor layers placed in-between two metallic electrodes.
Organic semiconductors have equally gained attention as strong light absorber and charge transport materials in organic solar cells, with whom flexible PV modules can be built. In recent years, organic semiconductors have also been key to the ground-breaking hybrid organic-inorganic perovskite solar cell technology, which is the hottest emerging photovoltaics technology and shows great potential for LED applications, too. Further into the invisible range of electromagnetic waves, terahertz photonics is a growing technological field for non-invasive diagnostics applications.
The ICP carries out R&D in the field of OLED, OPV, perovskite PV and non-linear optical crystals for terahertz photonics technology by employing multi-physics computer models and devising novel measurement systems. In the laboratory of the ICP, we fabricate OLEDs and novel solar cells on a small scale for R&D purposes and are setting up a terahertz photonics measurement system. We focus on device and material characterization methods by a combination of advanced measurement and simulation technology. In this ICP research topic we have been collaborating with international industrial and academic partners and also carry out Ph.D. projects. The spin-off company Fluxim AG is developing the Setfos and Laoss simulation software as well as the all-in-one measurement setup Paios in close collaboration with the ICP. This chapter gives an overview on ongoing R&D projects carried out in this interdisciplinary research field of the ICP.

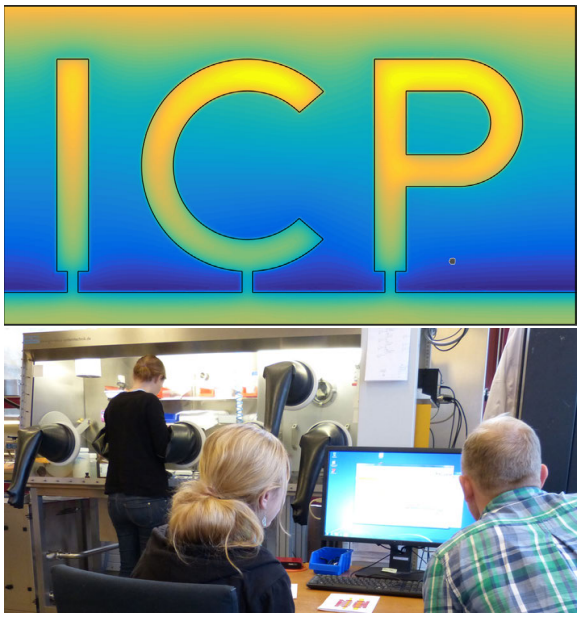

3.1 Optimization of solar cell metallic contacts

Thin-film solar cells and modules rely on transparent conductive oxides (TCO) to transport the generated current to external contacts. Since a few years a metallic mesh is used in combination with the TCO to improve the conductivity. At ICP numerical simulations are used to automatically optimize the current collection by minimizing both electrical losses and optical losses due to absorption and shadowing in the TCO and mesh.

Contributors: P. Losio, B. Ruhstaller
Partners: CSEM, EMPA, EPFL-PV-Lab, EPFL-LPI
Funding: Swiss Federal Office of Energy, CCEM
Duration: 2014–2017

Transparent conductive oxide (TCO) layers are usually used to transport the current generated in thin-film solar cells, however the layer conductivity is usually orders of magnitude lower than in metals thus leading to Ohmic losses. In recent times, a fine metallic conductive mesh is added on top of the TCO surface to improve the conductivity at the expense of a localized total loss of generated current due to shadowing.

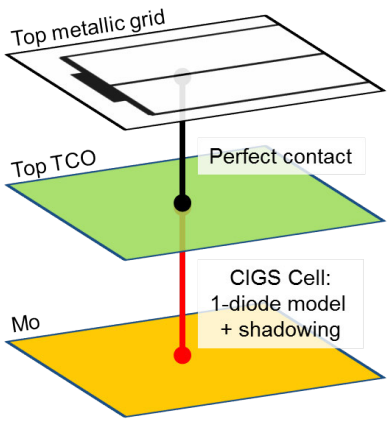

Fig. 1: Schematic representation of the model geometry, dimensionality and couplings.

The optimization of metallic meshes in combination with TCO layers requires the use of a computationally efficient 2D+1D FEM approach to correctly model the voltage distribution across the cell and the electrical losses as shown in Fig. 1. In principle it is possible to automatically optimize the topology and the shape of metallic contacting grids by using topology optimization algorithms used e.g. in civil engineering but adapted to the problem of efficiently collecting current from a surface minimizing shadowing. An intuitive optimization method is the Bidirectional Evolutionary Structural Optimization (BESO) method which was adapted to optimize electrical contacts. The optimization algorithm iteratively adds metal mesh elements to the top electrode at points where the Ohmic losses in the top TCO layer are highest. This approach is repeated until gains in current collection are compensated by losses due to shadowing and the efficiency of the cell cannot be increased any more. A first application was the optimization of contacting meshes for CIGS solar cells. The reference contact mesh and two optimized meshes are shown in Fig. 2. EMPA Dübendorf prepared the optimized meshes on CIGS solar cells and the improvement of performance could be confirmed experimentally: modifying the contact mesh allows an absolute improvement of the photovoltaic conversion efficiency of +0.3 % for both meshes.

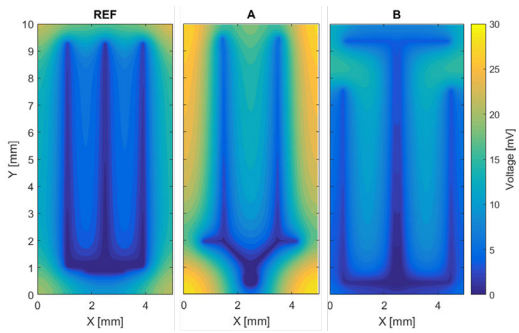

Fig. 2: Potential difference distributions on the top TCO for a reference contact and for two optimized contacts. A small potential difference indicates an optimized contact.

Compared to the reference the optimized contact-A reduces the shadowing losses at the cost of slightly higher Ohmic losses. Contact-B, on the other hand, allows to reduce the shadowing losses without increasing the Ohmic losses.

Literature:

[1] P. Losio, et al. *Evolutionary Optimization of TCO/Mesh Electrical Contacts in CIGS Solar Cells*, 32nd EUPVSEC, Munich, 2016.

3.2 Accurate determination of the optical properties of CIGS absorber materials

The accurate determination of the optical properties of CIGS absorber materials is fundamental to predict the solar cell performance. An improved model of the material properties was developed at ICP and the model predictions agree well with measured data.

Contributors: P. Losio, B. Ruhstaller
Partners: EMPA
Funding: Swiss Federal Office for Energy, CCEM
Duration: 2014–2017

Cu(In, Ga)Se_2 (CIGS) thin-film solar cells are promising for large-scale efficient PV applications. Therefore improving the accuracy of the predictions obtained from models of CIGS solar cells is important in the community, especially considering that light management in CIGS cells is a current topic of research. A fundamental aspect toward accurate modelling of the optical losses in CIGS solar cells is an accurate knowledge of the optical properties of the materials under study. Considering the freedom of modifying the relative Gallium and Copper content in the CIGS absorber material it is challenging to obtain precise optical data of the material.

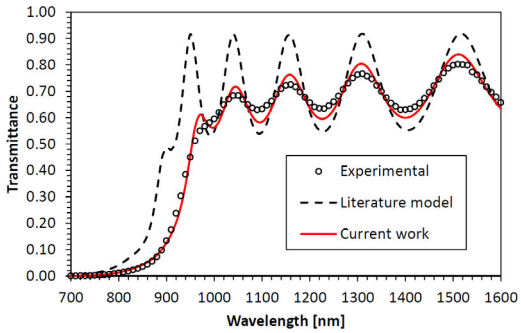

Fig. 1: Transmittance as a function of wavelength through a CIGS sample: measurements (circles) are compared with simulations (lines). The dashed line was computed using the most recent model from literature and the continuous line is based on the refined model developed in this project.

As part of this project, the best model available from literature [1] was implemented and compared with experimental data. Depth-resolved measurements of the Ga and Cu concentration in conjunction with the predicted optical parameters were used to simulate the EQE of selected CIGS solar cells prepared at EMPA. Surprisingly, the results did not match the experimental transmission and EQE curves as shown in Fig. 1-2. These findings combined with further work done at EMPA indicated a general mismatch between the literature model and experimental data. As a consequence work continued to improve the optical model of the CIGS material combining experimental efforts at EMPA and modeling efforts at ZHAW. Several single CIGS layers with uniform composition were prepared at EMPA and accurately measured to determine the bandgap. Using these data at ZHAW the complex refractive index dispersions were fitted by implementing a bandgap correction of the literature model and adding a phenomenological description of the partially incoherent light arising from the surface roughness of the layers. Finally using the improved model it was possible to achieve a good agreement between measured and simulated data as shown in Fig. 1 for one CIGS layer. The bandgap correction allows to match the experimental data at 950 nm and the phenomenological modeling of partial decoherence allows to correctly describe the amplitude of the fringes. Applying the corrected model to a full solar cell stack allows to accurately model the EQE, too, as shown in Fig. 2: the integrated current matches the experimental value within 0.5%.

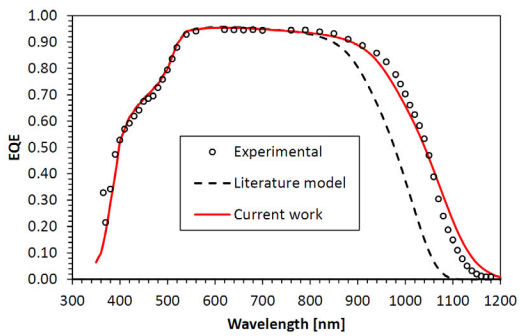

Fig. 2: EQE of a CIGS solar cell: measurements (circles) are compared with simulations (lines). The calculations take into account the depth-resolved Ga and Cu content of the absorber material. The dashed line was computed using the most recent model from literature and the continuous line is based on the refined model developed in this project.

Literature:

[1] S. Minoura, et al., J. Appl. Phys., 117 (19), 195703, 2015.

3.3 Bottom-up energy yield simulations for the optimization of PV modules

Photovoltaic cells are characterized at well-defined standard conditions, however PV modules in installations operate at a wide range of conditions. Simulating the energy yield of a photovoltaic module considering real outdoor conditions is a useful tool for supporting optimization.

Contributors: P. Losio, B. Ruhstaller

Partners: CSEM, EMPA, EPFL-PV-Lab, EPFL-LPI
Funding: Swiss Federal Office for Energy, CCEM, SNSF
Duration: 2014–2017

The energy yield of a photovoltaic module in an outdoor installation is influenced by several factors including weather, time of the year, geographical location, and orientation. These factors determine the light spectrum and intensity illuminating the solar cell and its operating temperature, which in turn strongly influence the power produced by the solar cell and its efficiency. Usually the energy yield of photovoltaic modules is assessed experimentally by long term outdoor measurements, however for optimization of the solar cell device structure it is useful to predict the energy yield using a bottom-up approach. To achieve this a model was developed taking into account the local weather, the geographical position, the device orientation and the device structure. Combining this information with measured EQE curves, IV curves and weather data, the energy yield of a solar cell can be estimated.

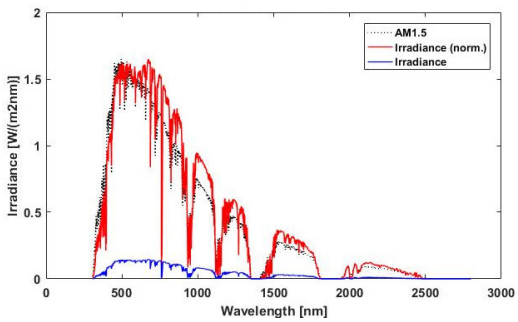

Fig. 1: Clear-Sky sun spectrum computed with SMARTS for the 14th January 2015 at 3PM in Zürich. The dotted line is the standard sun spectrum, the blue line is the computed spectrum and the red line is the computed spectrum rescaled to highlight the spectral shift toward red light.

Synthetic clear-sky sun spectra were generated based on the time of the year and geographical location using SMARTS [1] to take into account the atmospheric absorption and the red/blue shift of the spectrum as shown in Fig. 1. Then weather data consisting of integrated irradiance, temperature, wind, and pressure were obtained from MeteoSwiss (the Swiss Federal Office of Meteorology and Climatology), and they were used to rescale the clear-sky sun spectrum to the measured irradiance and to estimate the module temperature. Measured IV data together with temperature coefficients [2] were then used to predict the module power. The weather data originate from hourly measurements during one whole year thus allowing an accurate averaging of the performance. To show the capabilities of the tool, the energy yield of an high performance CIGS solar cell was simulated in Zürich and at Jungfraujoch taking weather data of 2015. Some results are shown in Fig. 2. Several cases were studied: cell kept at constant temperature e.g. ignoring the air temperature, cell at variable temperature, module without optimization and module after two optimizations.

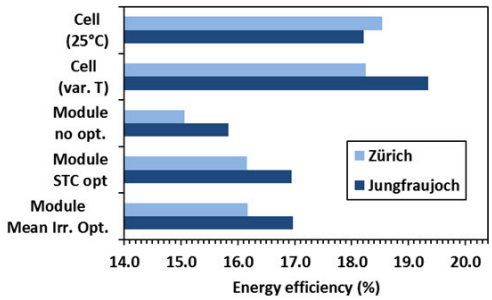

Fig. 2: Energy Yield simulations at two locations considering weather data for 2015 and based on a 20.4% CIGS solar cell.

In general the energy yield efficiency of a solar cell will be below the efficiency measured under standard test conditions, and the weather plays a major role in determining its performance.

Literature:

[1] C. Gueymard, Solar Energy, 71 (5), 325–346, 2001.
[2] A. Virtuani, 25th EUPVSEC, DOI 10.4229/25thEUPVSEC2010-4AV.3.83

3.4 Supporting the development of perovskite solar cells and OLECs with new measuring and simulation tools

Although perovskite solar cells emerged only in 2012, they have already reached conversion efficiencies of more than 22%, which is almost twice the conversion efficiency reached by organic solar cells. Available simulation tools are not able to satisfyingly reconstruct the electronic behavior of perovskite solar cells and organic light-emitting electrochemical cells (OLECs). ICP is developing improved measurement techniques and numerical methods to simulate ionic transport.

Contributors: E. Knapp, M. Neukom, B. Ruhstaller, A. Schiller
Partners: EMPA, Fluxim AG
Funding: CTI
Duration: 2016–2019

Perovskite solar cells are thin film devices in which the light absorbing layer consists of a perovskite structured organic-inorganic compound. Despite their comparatively late emergence, exciting high efficiencies have already been reached. Electronic investigation of perovskite solar cells showed unusual electronic properties like current-voltage hysteresis and a strong low frequency response. Similar properties are observed for OLECs. These electronic properties have been intensely discussed in the scientific community and are commonly attributed to mobile ions.

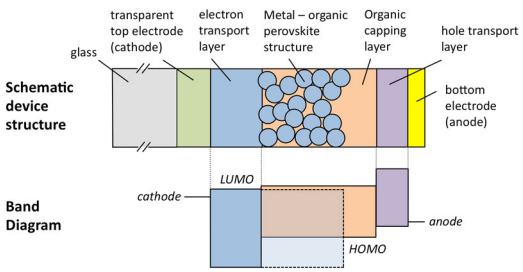

Fig. 1: Schematic buildup and qualitative band diagram of an exemplary perovskite solar cell.

The equations to model mobile ions are for the most part identical to those of free charge carriers. They however differ in the boundary conditions and the value for the mobility. This causes some challenges for the numerical methods. The free charge carriers are electrons and holes which quickly move through the device. Thus a high resolution in time is needed during the first microseconds of the simulation. On the contrary the mobility of the ions is commonly several orders of magnitude lower. This leads to a total time of many seconds up to several minutes until the steady-state solution is reached.

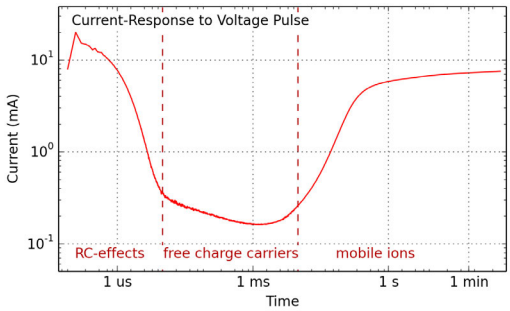

Fig. 2: Transient measurement of the current response to a voltage pulse of a perovskite solar cell. Only in logarithmic time scale the dynamics of free charge carriers and mobile ions can be illustrated which is the main challenge for measurement and simulation.

Similar problems occur for the experimental measurement of perovskite solar cells and OLECs. To fully characterize the devices, measurements from high to low frequencies are necessary. The frequencies can be so low, that the experiments take from several hours up to some days. One of the goals of this project is to perform measurements with several frequencies at once to save time.
The CTI project Perolec aims to develop new tools to tackle these challenges. ICP develops and evaluates the numerical methods and the measurement techniques. The collaboration with the ICP spin-off Fluxim allows for the implementation of the new tools into the simulation software Setfos and the integrated measurement solution Paios. Both are commercially available and widely used by customers. The research partner EMPA fabricates OLECs and perovskite solar cells, which are then measured at ICP and Fluxim to test and validate the new tools.
With the Perolec project ICP contributes to an emerging field in academic and industrial research.

3.5 Hysteretic IV-behavior of perovskite solar cells

Perovskite solar cells are arguably the most promising new technology among 3rd generation photovoltaic cells. While enormous progress has been achieved by testing different material compositions and optimization of manufacturing processes, there is still a lack of understanding of their fundamental physics. We use numerical simulation to test the hypothesis, that mobile ions cause novel transient effects that are unique for this technology. Our results confirm that a variety of those effects can be explained by ion transport and shed light on the impact of ion movement on cell performance.

Contributors: D. Bernhardsgrütter, M. Schmid
Partners: EPFL-LPI, EPFL-PV-Lab, EMPA-TFPV
Funding: SNSF
Duration: 2015–2018

Perovskite solar cells have attracted tremendous interest within the photovoltaic community over the last years. The technology is regarded as a promising candidate to compete with silicon solar cells in the near future. Indeed, the excellent optical and electrical properties of perovskite materials have boosted the efficiencies above 20% within less than 10 years of research. No other technology has achieved comparable results in such a short stretch and perovskite has the bonus of being a potential low-cost technology through low-temperature solution processing. While the achieved efficiencies suffice to compete with current technologies on the market, establishing long-term stability still entails large challenges.

Perovskite solar cells show unique transient effects as for example hysteresis in current-voltage scans, see Fig. 1a. Among other explanatory approaches, mobile ions have been proposed to play an important role for these hysteretic effects. We use numerical simulations to test this hypothesis. Our model comprises one dimensional drift-diffusion equations coupled with ion transport. The fully coupled system of equations is solved numerically in Comsol.

Our results indicate that hysteretic current-voltage curves can indeed be explained by ion migration. The ions are assumed to have very low mobility, thus they lag behind the voltage ramp. Depending on the scan direction, the ions either heap up at the boundaries of the perovskite material or they are predominantly uniformly distributed within the bulk of the perovskite. Accumulated ions at the boundary screen the internal electric field of the solar cell, which spoils electron and hole migration to the boundaries, cf. Fig. 1b. In case of massive ion accumulation at the boundaries, the probability for electrons and holes to recombine is increased which results in reduced current. In this way, the ion distribution affects the cell performance by favoring or hampering charge collection.

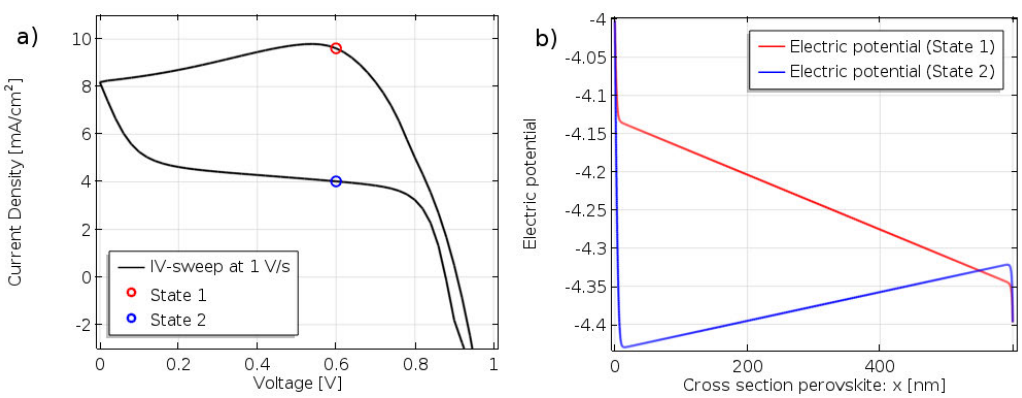

Fig. 1: a) Simulated IV-curve of a perovskite solar cell, where the sweep-rate is set to 1 V/s. The cell is initially held at steady state with applied voltage of 1 V. The scan direction is then from 1V to short circuit and back to open circuit. The cell performance is clearly reduced in the second part of the scan. b) Two snapshots of the electric potential during the IV-scan, both at the same applied voltage. At short circuit conditions, the internal electric field forces ions to migrate to the boundaries. Therefore, the ions are predominantly located at the boundaries at state 2, which affects the electric potential within the cell and ultimately drives the charge carriers to the wrong boundary, where they recombine.

3.6 High power ultra broadband and narrowband THz photonics based on molecular crystals

In this Korean-Swiss joint research project we aim at developing next generation high-power THz sources delivering ultra-broadband 0.1–15 THz and narrowband tunable radiation based on organic molecular crystals. ICP is developing theoretical and numerical models to support molecular crystal development at Ajou University and experimental high-power THz-wave generation demonstrations at PSI.

Contributors: M. Jazbinsek
Partners: PSI-SwissFEL, Ajou University
Funding: SNSF, NRF
Duration: 2016–2018

THz photonics is a growing research field and future scientific and technological breakthroughs rely strongly on advanced THz sources. Highly nonlinear optical molecular crystals offer unique advantages for THz-wave generation compared to alternative methods.

The main difficulty in developing optimized molecular crystals is due to the very broad expertise in both chemistry and physics needed, like molecular and crystal design and synthesis, large-area crystal growth, optical and nonlinear optical properties, material properties in the THz frequency range, THz-wave generation using different state-of-the-art laser systems and modeling to understand the structure-property relations. Based on the interdisciplinary collaboration of chemists, material scientists and physicists, deeper understanding of the correlation between the molecular and crystal structures and their nonlinear optical response is possible in this project [1].

The role of ICP in this project is to evaluate the correlation between molecular structures and physical properties, provide theoretical modeling of THz-wave generation and detection with molecular crystals, as well as parameter extraction and interpretation of broadband THz time-domain spectroscopy of molecular materials. For example, full optical and THz refractive index and absorption characterization of molecular crystals allow for theoretical evaluations of the expected THz electric field spectra and amplitude at various pump optical wavelengths and crystal thicknesses, see Fig. 1. This allows to optimize experimental parameters for THz-wave generation and also provides valuable feedback for molecular development and crystal engineering [2].

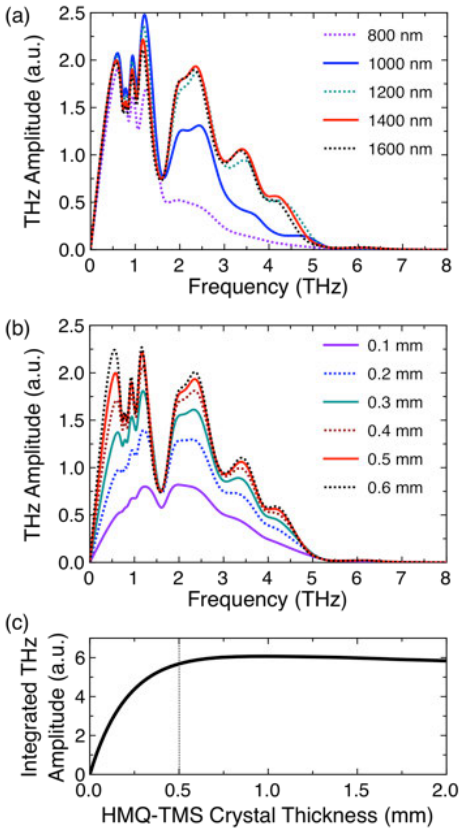

Fig. 1: Theoretical evaluation of THz electric field amplitude generated by optical rectification in HMQ-TMS using 150 fs pump pulses: (a) as a function of THz frequency for different pump wavelengths for a 0.5 mm thick crystal, (b) as a function of THz frequency at 1400 nm pump wavelength for different crystal thicknesses. (c) Integrated THz field amplitude vs. the generator crystal thickness at the pump wavelength of 1400 nm, where the phase matching is optimal [2].

Literature:

[1] S.H. Lee, M. Jazbinsek, C.P. Hauri, O-P. Kwon, Review Paper in CrystEngComm **18**, 7180–7203, 2016.

[2] S.H. Lee, S.J. Lee, M. Jazbinsek, B.J. Kang, F. Rotermund, O-P. Kwon, CrystEngComm **18**, 7311-7318, 2016.

4 Sensor and Measuring Systems

Nowadays almost every object of our daily life carries a functional coating. The coating not only determines the appearance, but also affects its properties such as its scratch or corrosion resistances. In order to ensure the quality of coatings, its thickness, homogeneity, material composition and adhesion properties have to fulfil certain standards. Previously, these coating properties often could only be determined in rather few individual samples. To minimize errors this often resulted in coatings being too thick, thus wasting material.
Lock-in thermography is a relatively new, non-destructive and non-contact testing method. In this case, a surface is thermally excited over a temporally changing heat flux. The resulting thermal radiation is recorded by infrared sensors and evaluated by means of computer algorithms. This allows one, for example, to detect invisible surface defects, whereby the depth range can be varied over the applied modulation frequency.
At ICP, lock-in thermography has been further developed for several years in the framework of numerous R&D projects. For example, in cooperation with the industrial partners J. Wagner, Oerlikon Metco and AkzoNobel the CoatMaster, was developed to measure coating thicknesses. The CoatMaster, is commercialized by the ICP Spin-Off Winterthur Instruments AG. In addition, ICP uses lock-in thermography to detect skin diseases. The resulting, patented Dermolockin process is commercialized through the ICP Spin-Off Dermolockin GmbH.

4.1 Measuring thermal coating resistance of turbine blades

Thermal barrier coatings (TBC) protect turbine blades against heat and mechanical stress. Due to uncontrollable process parameters, the thermal coating resistance varies during the production of turbine blades. Currently, the resistance is measured by a visible inspection of microscopic cross-section images. This is very labour intensive and requires the destruction of production samples. Therefore, we investigated a new, fast and non-destructive measurement approach using impulse thermography. We showed that it's possible to reliably measure the thermal coating resistance if the effusivity of the substrate is known.

Contributors: A. Bariska, N. Reinke, S. Hauri
Partners: Winterthur Instruments AG, Oerlikon Metco AG
Funding: CTI
Duration: 2015–2017

TBC consist of two layers: first a bond coat (nickel alloy) is applied to the steel substrate and then the functional top coat (yttrium stabilized zirconia, YSZ) is applied onto the bond coat. The two most important factors governing the protective function are the porosity and the thickness of the YSZ coating. In order to compare the barrier properties of two different coatings these two parameters have to be quantitatively combined. This combination is, however, difficult as the influence of the porosity on the thermal barrier property is dependent on the microstructure of the porosity.

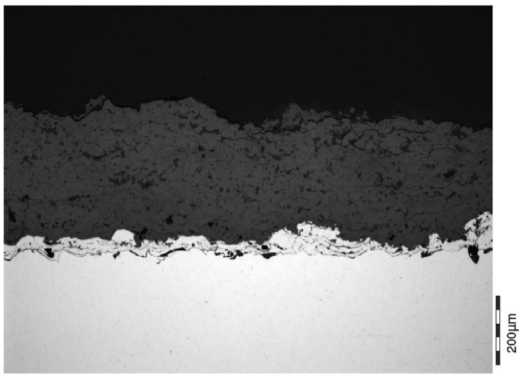

Fig. 1: Polished cross-section image of a TBC consisting of a bond coat (middle) and the top coat (top) on a steel substrate (bottom). Source: Oerlikon Metco AG, Wohlen.

Instead of using microscopic cross-section images as shown in Fig. 1 to determine the porosity and the thickness we used the impulse thermography-based CoatMaster measurement system to directly measure the thermal properties of the TBC. We assume, as a simple approximation, a constant heating power on the outside and a constant cooling power on the inside of the turbine blade. The temperature difference ΔT and the heat flow θ through the coating are constant and related, via a material parameter called thermal coating resistance R_{th}, with the formula $\theta = \Delta T / R_{\mathrm{th}}$. To make the values independent of the area we have to use the heat flux density in $\mathrm{W/m^2}$. The thermal coating resistance is therefore given in $(\mathrm{Km^2})/\mathrm{W}$. With the CoatMaster measurement system, we can directly measure the thermal propagation time of a coating τ (unit: s). If the thermal effusivity ϵ (units: $\mathrm{J/(m^2K\sqrt{s})}$) of the coating is known and the thermal propagation time is measured, the thermal coating resistance can be calculated with $R_{\mathrm{th}} = \sqrt{\tau}/\epsilon$.

In a series of measurements we could show that it is possible to reliably measure the thermal coating resistance with a fast and nondestructive measurement approach. A selection of measurements is given in Tab. 1.

Sample	Average Coat Thickness	Top Coat Porosity (image analysis)	Thermal Coating Resistance (absolute)	Thermal Coating Resistance (relative)
270	160µm			
284	140µm	4%	169 µKm²/W	75%
285	270µm	4%	225 µKm²/W	100%
286	328µm	1.9%	-	-
287	150µm	11.3%	221 µKm²/W	98%
288	228µm	11.1%	317 µKm²/W	141%
289	356µm	11%	-	-
290	75µm	15%	242 µKm²/W	108%
291	340µm	17.9%	-	-
292	280µm	15%	576 µKm²/W	256%

Tab. 1: Thermal coating resistance measured with the CoatMaster system.

4.2 Charge carrier dynamics in organic electronic devices

This project employs different layer architectures such as organic light-emitting diodes (OLEDs), solar cells and monopolar devices in order to study charge carrier transport. For this purpose we investigate new and improved measurement techniques in experiment as well as by numerical simulation. We develop reliable parameter extraction methods that are supported by numerical simulations.

Contributors: S. Züfle, E. Knapp, M. Regnat, B. Ruhstaller
Partners: Universität Augsburg
Funding: SNSF, DFG
Duration: 2015–2018

The most important transport parameter in organic electronic devices is the charge carrier mobility, which is usually obtained from monopolar devices. However, in multi-layer devices, bipolar charge transport as well as recombination and injection losses complicate the situation. Thus, new approaches to distinguish between different processes, to unambiguously assign extracted parameters to a specific layer and charge species, and to reliably determine these parameters are needed. By combining new experimental methods with drift-diffusion modeling we aim to achieve these goals.

A promising technique for the determination of the charge carrier mobility is the CELIV (charge extraction by linearly increasing voltage) technique performed on MIS-diodes (metal-insulator-semiconductor). This type of layer stack can be fabricated by adding an insulating layer on top of the material for investigation, thereby ensuring monopolar behavior. We have found that bilayer OLEDs employing a polar electron transport layer (ETL) show a voltage regime where they behave like a MIS-diode in accumulation. Therefore the MIS-CELIV technique can be employed to determine the hole mobility in the hole transport layer (HTL).

Fig. 1 shows an exemplary MIS-CELIV measurement on a polar OLED stack consisting of ITO/PEDOT:PSS/NPD/Alq3/Ca/Al. The peak position is related to the charge carrier mobility, and the curves show a strong temperature dependence. From an Arrhenius-analysis of the extracted mobility values we obtain the thermal mobility activation of the hopping transport. This claim is tested by drift-diffusion simulations of the device carried out with Setfos (Fluxim AG, Feusisberg), where the polar ETL is described by adding doped sheet charge layers in the simulated stack.

From the modeling we can give recommendations on how to perform the measurement in order to most accurately determine the mobility. Furthermore, we investigate how reliably the mobility thermal activation can be extracted. From reanalysis of simulations where this activation energy was varied we deduce a correction factor, which can then be applied to measured data.

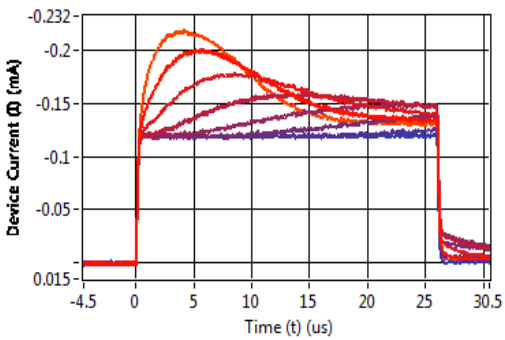

Fig. 1: MIS-CELIV measurement at varied temperatures. The transient peak position is related to the temperature-dependent hole mobility.

4.3 Fruitful collaboration leads to homebuilt cryostat

As an ICP spin-off, Fluxim is still closely collaborating with our institute. Recently, ICP helped developing a cheap alternative to expensive commercial cryostats. The ability to cool and heat LEDs and solar cells while measuring electronic properties is improving their research. Big parts of such collaborations are based on synergy effects, where both partners are contributing to the same projects and are working toward the same goals.

Contributors: M. Krajewski, S. Züfle, M. Neukom
Partners: Fluxim AG
Funding: Fluxim AG
Duration: 2014–

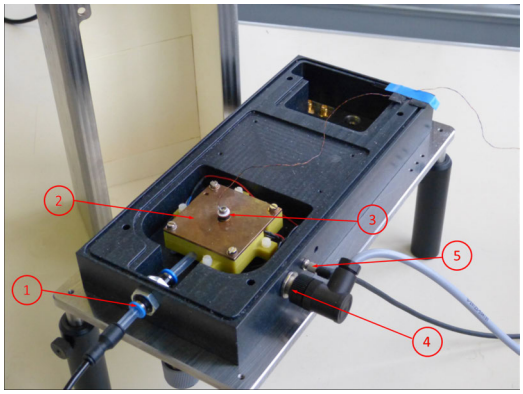

Fig. 1: Inside view of the homebuilt cryostat. Image adapted from ref. [1]

Typical organic light-emitting diode (LED) and solar cell measurements such as current-voltage characteristics or impedance spectroscopy are getting much more powerful when measuring at different temperatures, especially below 0 °C. In this way, information about barriers and trap energies can be extracted which leads to a deeper understanding of the devices and physics happening inside them. With our homebuilt cryostat shown in Fig. 1, temperatures close to the boiling point of nitrogen (-196 °C) can be achieved, which is done by running vaporized nitrogen through the tube (1). The device is placed on the cooled copper plate (2), and to investigate the cooling controller behaviour, an external temperature sensor (3) is placed on it for testing purposes. The heating plate and a built-in temperature sensor are connected via the connectors (4) and (5). With the heating plate, a more precise controlling is possible and temperatures up to 80 °C can be reached. Therefore, the overall temperature range at which devices can be measured is roughly -170 °C to 70 °C.

The cryostat is one of several projects resulting from a collaboration between the ICP and Fluxim. Not only measurement equipment is developed in this way, but also software. Fluxim, as a company that operates in the private sector, has a strategic interest in making knowledge, that was gathered during these projects, available to third party companies and other research units outside the scope of the projects in which ICP directly participates. Thus, there is extra effort needed to polish, port and integrate new software pieces and measurement system parts into the products of Fluxim. If ICP staff is involved in walking this extra mile as it is the case for the homebuilt cryostat, this effort is commissioned through the Fluxim Research and Development Support project. This includes tasks like making the software more stable, more flexible and faster, the hardware more reliable, more accurate and more economic and most of all in both cases more user friendly and accessible. As an outcome, a lot of reusable software and hardware is made available in a more powerful and convenient way. The ICP immediately profits from this, as it can make use of the products in subsequent R&D projects, letting Fluxim take care of the maintenance and fully concentrate on the new tasks at hand. With a symbiosis like this, less of the gained knowledge gets lost over time or stays inaccessible in unmaintained private software archives or in measurement tables.

Literature:

[1] O. Keller, R. Meier, *Modellbasierter Reglerentwurf für die Temperaturregelung eines Kryostaten*, supervisors: K. Pernstich, O. Fluder (IMS), semester project, 2015.

4.4 Solar-Controller optimieren mit Simulink-Polysun Cosimulation

Ob die Heizung in einem Gebäude energetisch optimal läuft, kann der Betreiber des Gebäudes oft nur an den Energiekosten ablesen. Leider zeigt sich in der Praxis, dass die Planwerte oft weit verfehlt werden. Im Planungstool kann man Abhilfe schaffen, in dem die Standardregler auch für die Entwurfsphase angeboten werden, so dass in einem späteren Schritt die Übertragung in die Praxis gut funktioniert.

Contributors: A. Witzig
Partners: Siemens Schweiz AG
Funding: Vela Solaris AG
Duration: 2016–

Die Steuerung gebäudetechnischer Energiesysteme ist für die Maximierung des Solarertrags sowie für die Optimierung der Anlageneffizienz von grösster Bedeutung. In realen Projekten zeigt sich jedoch, dass die Programmierung der Steuerung in der Planung und Projektierung oft nicht mit der effektiv in der Realisierungsphase umgesetzten Steuerung übereinstimmt. Das vorausgesagte gute Systemverhalten wird damit oft nicht erreicht. Bis anhin konnten im Simulationstool Polysun zwar mit einem programmierbaren Regler nutzerspezifische Regelkonzepte abgebildet werden, eine 1:1 Repräsentation von Spezialreglern wurde jedoch nicht angeboten. Im gemeinsamen Projekt mit dem Regelungshersteller Siemens wurde eine Kopplung der Siemens-internen Matlab/Simulink Routinen an die dynamische Simulation in der Standardsoftware Polysun entwickelt. Dabei liegt die Herausforderung darin, dass zwei dynamische Simulationsstränge parallel laufen und in regelmässigen Abständen ein konsistenter Zustand geschaffen werden muss. Die relevanten Simulationsdaten werden alle 3 Minuten abgeglichen, was sich für die untersuchten Beispiele als ausreichend genau herausgestellt hat. Wie in Fig. 1 dargestellt werden bei Erreichen des Synchronisierungs-Zeitpunkts (1) die Sensorsignale von Polysun (Anlagenmodell) zu Simulink (Regler) übertragen. Dann werden (2) die Übergabewerte des Reglers berechnet und (3) an Polysun zurück übertragen, so dass sie für die Anlagen-Simulation für die weiterführende Berechnung (4) unmittelbar berücksichtigt werden. Die Polysun-Simulation führt dabei mit variablem Zeitschritt so viele Simulationsschritte aus, bis zum Zeitpunkt t+3 min die nächste Kopplung initiiert wird. Parallel dazu wird dann (5) auch der restliche Teil des Reglers (zeitkontinuierliche Integratoren) für den nächsten Cosimulations-Zeitschritt simuliert. Die Möglichkeit, einen externen Algorithmus zu koppeln, ist für professionelle Anwender auch deshalb von grossem Interesse, da firmeneigene IP dadurch ideal geschützt werden kann. Die neuen Kopplungsmöglichkeiten ergänzen bereits bestehende Schnittstellen und setzen einen zusätzlichen Fokus auf die Steuerung von Solaranlagen und Heizung/Lüftung/Klima (HLK)-Systemen. Weitere Anwendungsmöglichkeiten bestehen in der Eigenverbrauchsoptimierung von Anlagen, in denen die Wärmeversorgung mit der Nutzung von photovoltaischer Solarenergie kombiniert wird.

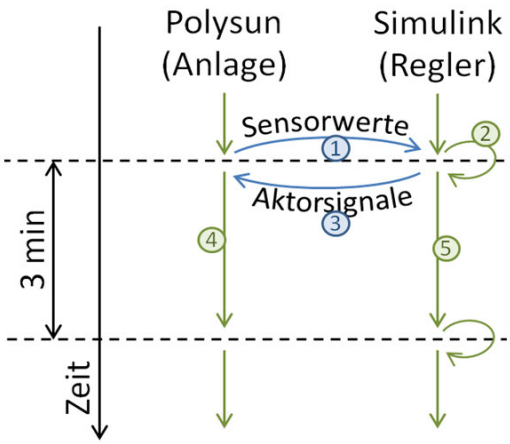

Fig. 1: Ablaufschema der Cosimulation mit Polysun und Matlab/Simulink.

Literatur:
[1] A. Wolf, R. Kurmann, C. Gähler, A. Witzig, *Solar-Controller optimieren mit Simulink-Polysun Cosimulation*, OTTI-Symposium Thermische Solarenergie, Bad Staffelstein D, 2017.

4.5 Robuste und kosteneffiziente Auslegung von thermischen Solaranlagen

Mit thermischen Solaranlagen kann pro Fläche mehr Solarenergie geerntet werden als mit Photovoltaik. Die Anlage muss jedoch gut mit dem Warmwasserbedarf abgestimmt werden. Bei der Dimensionierung der Rohrleitungen müssen verschiedene weitere Punkte beachtet werden. Um die Planungskosten und die Risiken zu minimieren, werden diese Aufgaben mit einer Simulationssoftware unterstützt.

Contributors: A. Witzig, H. Sotnikova, R. Eismann
Partners: ETHZ, Vela Solaris AG
Funding: Swiss Federal Office of Energy
Duration: 2016–

Solarkollektoren wandeln die eingestrahlte Sonnenstrahlung in Wärme um. Die meisten Anlagen speichern die Wärme in einem grossen Wassertank. Während für die energetische Dimensionierung leistungsfähige Simulationsprogramme zur Verfügung stehen [1], fehlen die entsprechenden Programme zur thermohydraulischen Dimensionierung weitgehend. Es war bisher beispielsweise nicht möglich, die Rohrdimensionen und die Pumpe des Solarkreislaufs präzise und kostenoptimal auszulegen. In einem ETH-Forschungsprojekt wurden die Algorithmen zur Auslegung entwickelt und mit entsprechenden Messungen die Simulationsparameter bestimmt [2,3]. In der letzten Phase des Projektes wurde gemeinsam mit dem ICP und der Firma Vela Solaris ein industrietaugliches Simulationsverfahren entwickelt [4].

Eine spezielle Herausforderung ist der Betriebszustand, den man Stagnation nennt: Dieser tritt typischerweise nach längeren Schönwetterperioden im Sommer auf, wenn die thermischen Speicher ihre Maximaltemperatur erreicht haben. In diesem Fall werden die Pumpen gestoppt. In der Folge erhitzen sich die Kollektoren über den Siedepunkt des Wärmeträgermediums hinaus. Die hydraulische Anlage kann dies gut verkraften, falls gewisse Regeln eingehalten werden. Der Dampf entsteht im Kollektor und durch die Rohrleitungen wird der Rest des flüssigen Wärmeträgermediums in die Anlagen gepresst. Ein Druckausgleichsbehälter (Expansionsgefäss) bietet genügend Volumen und hält den Druck auf einem konstanten Niveau. Mit dem neuen Simulationsverfahren werden die auf Faustregeln beruhenden bisherigen Dimensionierungsvorschriften verfeinert (Fig. 1). Das resultierende Vorgehen ist kosteneffizient und sicher.

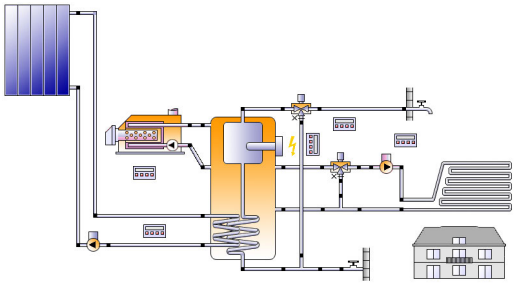

Fig. 1: Thermische Solaranlage für Warmwasser und Gebäudeheizung: Hydraulikschema im Simulationsprogramm Polysun.

Literatur:

[1] http://www.polysunsoftware.com
[2] R. Eismann, A. Witzig, *Programm THD - Thermohydraulisches Dimensionierungsprogramm für Solaranlagen*, Schlussbericht BFE, 2016.
[3] R. Eismann, *Thermohydraulische Dimensionierung von Solaranlagen*, Springer, 2017.
[4] R. Eismann, F. Föller, A. Witzig, *THD - Thermohydraulisches Dimensionierungsprogramm für Solaranlagen*, OTTI-Symposium Thermische Solarenergie, Bad Staffelstein D, 2017.

4.6 Entwicklung eines Handgeräts zur zerstörungsfreien Prüfung von Beschichtungen im Baubereich

Die aktuelle Technik zur Prüfung von Schichtdicken führt zu Schwachstellen in der Schutzschicht. Es wird die Oberfläche angebohrt um die Dicke mit einem Messinstrument zu bestimmen. Ziel dieser Arbeit war es, ein Messgerät zu entwickeln, welches portabel ist und die Beschichtung nicht verletzt. Dies konnte anhand von spezifisch induzierter Wärme realisiert werden. Es wurde ein funktionierender Prototyp hergestellt und an Materialien der Firma Franken Systems GmbH erfolgreich getestet.

Students: A. Bleuler, N. Salihi, J. Storskogen

Category: Bachelor of Science, Bachelorarbeit
Mentoring: A. Bariska, N. Reinke
Handed In: Februar 2017

Während einer ersten Phase im Rahmen eines Semesterprojekts wurden verschiedene Möglichkeiten getestet, die Dicke von Beschichtungen zerstörungsfrei zu messen. Als optimale Lösung erwies sich eine thermische Schichtprüfung, welche eine Messung im mm-Bereich ermöglicht. In der Fig. 1 ist ersichtlich, dass die Oberflächen unterschiedliche Infrarot (IR)-Strahlung abstrahlen. Die Proben wurden mit einer Halogenlampe erwärmt und während eines Zeitraums von 30 Sekunden wurde die IR-Strahlung gemessen.

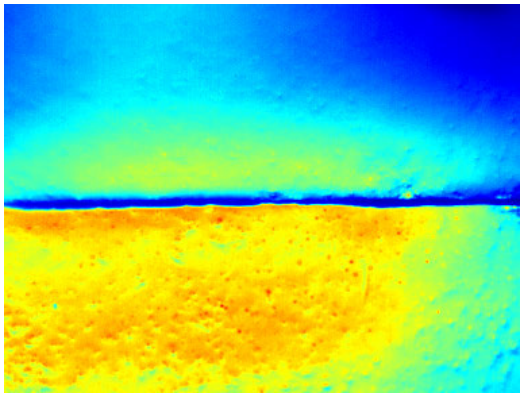

Fig. 1: Unterschiedliche Wärmeverteilung der induzierten Wärme auf der Kunststoffbeschichtung Frankosil 1K von Franken Systems GmbH. Oben mit 110 g/m^2 und unten mit 160 g/m^2 Flies.

In der zweiten Phase, welche im Rahmen einer Bachelorarbeit stattfand, wurde ein funktionierender Prototyp entwickelt. Im Vordergrund stand hierbei die Handhabung des Geräts. Es musste zwingend als Handgerät realisiert werden um ortsunabhängige Messungen durchführen zu können. Hierfür wurden diverse Aufbauten anhand von Messungen getestet und in mehreren Schritten zum funktionsfähigen Prototypen entwickelt (Fig. 2).

Fig. 2: Prototyp mit Illustration des Messvorgangs. Links wird Infrarotlicht in die Beschichtung gestrahlt und rechts die reflektierte Infrarotstrahlung detektiert. Diese wird der Schichtdicke zugeordnet, welche mittels Display ausgegeben wird.

Das Messprinzip basiert auf einer rechteckförmigen optischen Erwärmung sowie einer Messung der von der Oberfläche abgestrahlten IR-Strahlung. Die detektierten Temperaturen werden in Relation zur Zeit gesetzt und können so der entsprechenden Schichtdicke zugeordnet werden. Diese innovative Methode ermöglicht es materialunabhängig Beschichtungdicken zerstörungsfrei zu messen. Hierbei hat der Untergrund keinen Einfluss. Somit können sogar Beschichtungen auf Holz oder Gestein mit einer Genauigkeit von 0.1 mm ausgemessen werden. Der aktuelle Prototyp wird in einem KTI-Projekt in Zusammenarbeit mit dem ICP weiterentwickelt, um einerseits die Zuverlässigkeit der Messergebnisse zu optimieren, deren Auswertung und Interpretation zu erleichtern, und andererseits weitere Anwendungsgebiete zu erschliessen.

4.7 Prozessregelung einer Beschichtungsanlage für OLEDs

In seinem hauseigenen Labor stellt das ICP u. a. organische Leuchtdioden und Solarzellen her. Dazu müssen unterschiedliche Schichten in einem thermischen Verdampfungsprozess in einer Vakuumkammer aufgebracht werden. Dieser Beschichtungsprozess lässt sich nur unbefriedigend manuell steuern. Daher wurde ein Regler entworfen, der den Beschichtungsprozess besser steuert, als dies von Hand möglich ist.

Students: O. Acar, F. Feddersen

Category: Bachelor of Science, Semesterprojekt
Mentoring: K. Pernstich, O. Fluder (IMS)
Handed In: Dezember 2016

Bei der Herstellung von organischen Leuchtdioden und Solarzellen wird das Ausgangsmaterial auf eine bestimmte Temperatur erwärmt, bei der es in die Gasphase übergeht (Sublimation). Ein spezielles Messgerät misst die Aufdampfrate, mit der sich das Material als Film abscheidet. Diese Aufdampfrate soll auf einen bestimmten Wert eingestellt und während des gesamten Beschichtungsprozesses konstant gehalten werden.
Dafür wurde eine Kaskadenregelung entworfen (Fig. 1). Der innere Regler kontrolliert die Temperatur des Tiegels, und der äussere Regler gibt den Temperatursollwert entsprechend der aktuellen Aufdampfrate vor. Da während dem Aufheizen des Tiegels die Aufdampfrate immer null ist und daher die Temperatur nicht richtig geregelt werden kann, wurde eine Stoss-freie (engl. bump-less) Umschaltung zwischen Temperatur- und Ratenregelung eingebaut.
Bei der Konzeption des Reglers hat eine Systemidentifikation ergeben, dass das Temperaturverhalten als PT1-Glied ausreichend genau beschrieben werden kann, während die Aufdampfrate ein schwingungsfähiges PT2-Verhalten zeigt. Nach der Reglerauslegung mit Matlab wurde der Regler in LabView implementiert und an der Anlage getestet.

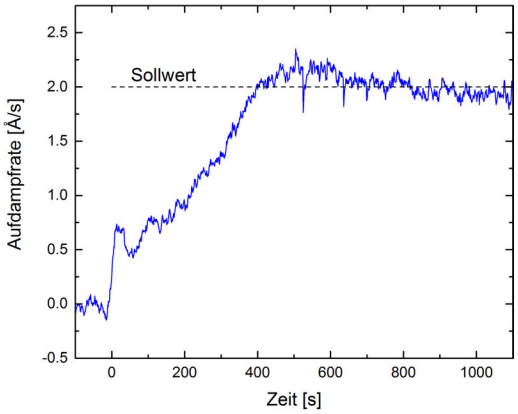

Fig. 2: Aufdampfrate für einen Alq3-Film. Die gewünschte Rate von 2 Å/s wurde sehr genau geregelt.

Fig. 2 zeigt die gewünschte und gemessene Aufdampfrate für die Abscheidung eines Alq3-Films. Die gewünschte Aufdampfrate von 2 Å/s wurde innerhalb von 400 Sekunden erreicht und blieb innerhalb enger Grenzen konstant. Diese Stabilität wird bei einer manuell gesteuerten Beschichtung selten erreicht.

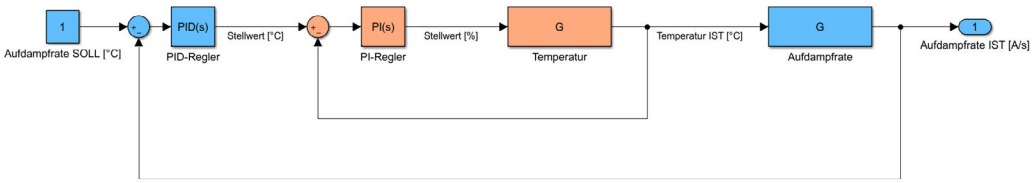

Fig. 1: Blockschaltbild der Kaskadenregelung für Temperatur (orange) und Aufdampfrate (blau).

4.8 Tieftemperatur-Messplatz mit Peltier-Elementen

Für Lebensdauerstudien an organischen Leuchtdioden und Solarzellen müssen diese Bauteile oft auf Temperaturen bis -40℃ abgekühlt werden. Diese Temperatur kann mittels Peltier-Elementen komfortabel erreicht werden. In diesem Semesterprojekt wurde ein Prototyp eines solchen Peltier-Kühlgeräts simuliert, entwickelt, aufgebaut und getestet.

Students: A. Meier, R. Ropelato

Category: Bachelor of Science, Semesterprojekt
Mentoring: K. Pernstich, O. Fluder (IMS)
Handed In: Dezember 2016

Ausgehend von einer Schätzung der benötigten Kühlleistung wurde ein passendes Peltier-Element ausgewählt und ein CAD-Entwurf des gesamten Messaufbaus entwickelt, siehe Fig. 1. Basierend auf dieser CAD-Zeichnung wurde mit Hilfe des Finiten-Elemente-Programms COMSOL Multiphysics das thermische Verhalten des Prototypen simuliert. So konnte die erreichbare Temperatur des Proberaums vorausgesagt, sowie Bereiche mit grossen thermischen Verlusten identifiziert werden. Aus diesen Simulationen liessen sich Verbesserungsvorschläge im Aufbau ableiten.

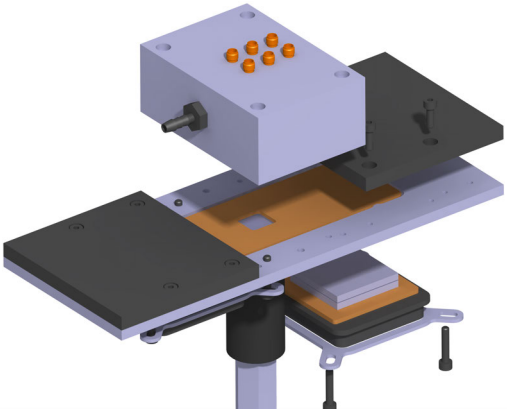

Fig. 1: CAD-Rendering des Peltier-Kryostaten.

Das Peltier-Kühlgerat muss zwingend die zu untersuchenden Proben von der Raumluft abschirmen, um eine Kondensation des Wassers in der Luft bei tiefen Temperaturen zu vermeiden. Dazu wurde eine Abdeckung entworfen, dank der sich im Probenraum ein Vakuum erzeugen lässt. So lässt sich eine Kondensation vermeiden. Weil die zu untersuchenden Proben jedoch auch Licht ausstrahlen bzw. aufsammeln, musste auch ein vakuumdichtes Fenster eingebaut werden. Die Kühlung der Probe verschlechterte sich dadurch nicht wesentlich.

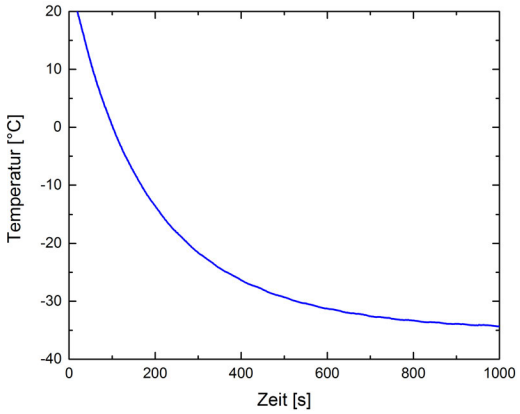

Fig. 2: Gemessener Verlauf der Probentemperatur.

Fig. 2 zeigt den Temperaturverlauf bei ersten Testmessungen. Die gewünschte Temperatur von -40℃ wurde fast erreicht. Mit den Verbesserungsvorschlägen aus den thermischen Simulationen sollte die gewünschte Temperatur von -40℃ erreicht werden. Diese Vorschläge, zusammen mit weiteren Verbesserungen, werden im Rahmen einer Bachelorarbeit umgesetzt.

5 Seamless Learning

Lernen findet in der Regel in einem komplexen Umfeld statt. Seamless Learning – im Deutschen meist als *durchgängiges Lernen* übersetzt – verbindet die verschiedenen Lernphasen und überbrückt die Gräben, die sich durch einen Kontextwechsel ergeben. Die neuen didaktischen Methoden bedienen beispielsweise die Schnittstelle zwischen Berufsschule und Ingenieurausbildung und helfen bei der Umsetzung des erworbenen Wissens an der Arbeit. Oft stützen Seamless-Learning-Konzepte auf digitale Lehrformen und mobile Endgeräte ab. Im Physik- und Mathematikunterricht können Computersimulationen unterstützend eingesetzt werden.
Die bisher präsentierten Beiträge im Forschungsbericht beschreiben wissenschaftliche Arbeiten mit ICP-Beteiligung, die im vergangenen Jahr durchgeführt wurden. Mit Blick in die Zukunft soll hier ein interdisziplinäres Tätigkeitsfeld vorgestellt werden, in welchem das ICP die Leistungsbereiche Forschung und Lehre verbindet und bei der ZHAW-internen und internationalen Vernetzung eine aktive Rolle spielt.
Die Internationale Bodensee-Hochschule IBH hat im 2016 erstmals Projekte in grösseren Themenclustern ausgeschrieben. In sogenannten *Labs* werden eine nachhaltige Vernetzung von Wissenschaftlern sowie eine enge Einbindung von nichtakademischen Partnern in Forschungsprojekte angestrebt. Die ZHAW hat sich mit weiteren Konsortiums-Partnern für den Themencluster *Bildungs- und Wissensraum Bodensee* beworben und im Ideenwettbewerb den Zuschlag bekommen. Mit dem IBH-Lab *Seamless Learning* werden in den Jahren 2017 bis 2020 wiederverwendbare Lernobjekte für den Unterricht in Technik und Wirtschaft erarbeitet. Stufenübergreifend werden computergestützte Lernmethoden und fachdidaktische Konzepte eingesetzt und deren Effekt auf die Wissensvermittlung untersucht.
Gemeinsam mit dem Zentrum für Innovative Didaktik ZID an der School of Management and Law leitet das ICP das Seamless-Learning-Lab. Unter dem Schirm dieses Labs werden rund 10 Projekte durchgeführt. Das Konsortium umfasst die folgenden Institute und Hochschulen:

- ZID Zentrum für Innovative Didaktik, School of Management and Law, ZHAW
  Prof. Dr. Claude Müller Werder, Jennifer Erlemann, Dr. Christian Rapp

- ICP Institute of Computational Physics, School of Engineering, ZHAW
  Dr. Andreas Witzig, Dr. Matthias Schmid

- IAMP Institut für Angewandte Mathematik und Physik, School of Engineering, ZHAW
  Dr. Elisabeth Dumont, Prof. Hans Fuchs

- IMS Institut für Modellbildung und Simulation, Fachhochschule St. Gallen
  Dr. Katrin Hügel

- Professur für ingenieurs- und naturwissenschaftliche Grundlagen mit Propädeutik, Hochschule Albstadt-Sigmaringen
  Prof.Dr. Carola Pickhardt

- Fakultät Informatik, Hochschule Konstanz Technik, Wirtschaft und Gestaltung (HTWG)
  Prof. Dr. Rebekka Axthelm, Prof. Dr. Ralf Schmikat

- PWO Institut für Produktionsmesstechnik, Werkstoffe und Optik, NTB Interstaatliche Hochschule für Technik Buchs (HTB)
  Prof. Dr.-Ing. Michael Marxer

- Institut für Wirtschaftspädagogik, HSG Universität St. Gallen
  Prof. Dr. Bernadette Dilger

Im vergangenen Jahr haben ICP und ZID die Strukturen geschaffen, so dass im 2017 erste Projekte starten und die weiteren Vorhaben geplant werden können. Thematisch werden Beiträge zum aktuellen Technologieschub in der Didaktik ausgearbeitet. Dabei wird mit der engen Anbindung an die Ingenieurausbildung der Realitätsbezug gewahrt und für eine nachhaltige Umsetzung in der Praxis gesorgt. Gerade die als schwierig angesehenen Fächer Mathematik und Physik stellen besondere Anforderungen an die Konzeption und Gestaltung moderner Lehr- und Lernszenarien.
Das IBH-Lab *Seamless Learning* reagiert auf den zeitlichen Wandel des Lernens und Lehrens. Neuerdings haben Lernende mithilfe von leistungsfähigen Laptops und Mobiltelefonen die Möglichkeit, überall und zu jedem Zeitpunkt zu lernen. Technologien entwickeln sich derart rasant, dass ein lebenslanges Lernen unumgänglich geworden ist. Seamless Learning hilft, bestehende Schranken zu überwinden, beispielsweise an der Schnittstelle zwischen der Berufsbildung und dem Studium an der Fachhochschule. Übergreifende Angebote wecken Interesse am Ingenieurstudium und helfen bei der Vorbereitung und Selektion zukünftiger Studierenden. Ein weiteres Beispiel für die Anwendung des *Seamless*-Konzepts ist der Transfer der wissenschaftlich-technischen Lerninhalte in die Praxis.
Das Konsortium ist entsprechend den Regeln des IBH länderübergreifend aufgestellt und auch ZHAW-intern breit abgestützt: Das Zentrum für Innovative Didaktik an der School of Management and Law hat dabei eine Schlüsselrolle. Andererseits ist auch das Institut für Angewandte Mathematik und Physik IAMP mit seiner langjährigen Lehrtätigkeit in den Fokusthemen gut eingebunden. IAMP und ICP können ihre Kompetenzen in Physik, Mathematik und Simulationstechnik und die Fachdidaktik-Kenntnisse optimal einbringen und weiterentwickeln.
Unabhängig von der Bewerbung um die IBH-Lab-Leitung hat das ICP im Jahr 2016 viel in die Didaktik investiert: Die grosse Mehrheit der jungen ICP-Dozenten haben den von der PH Zürich durchgeführten CAS Hochschuldidaktik besucht. Wir gratulieren Christoph Kirsch, Rebekka Axthelm, Matthias Schmid, Mojca Jazbinsek und Kurt Pernstich zum erfolgreichen Abschluss! Die erarbeiteten Portfolios und die Schlusspräsentationen dokumentieren nicht nur den reichhaltigen Inhalt der Weiterbildung, sondern haben auch in der gemeinsamen Präsentation mit den Absolventen des IAMP zu sehr interessanten Gesprächen und weiterführenden Projekten geführt. Mehrere Ideen können im Rahmen der von der School of Engineering geförderten Pilotprojekte *Digitale Lehrformen* in den Jahren 2017 und 2018 realisiert werden.
Die Aktivitäten zeigen erste Früchte der langfristigen Strategie eines akzentuierten Engagements des ICP in der Lehre. Es ist ein Gewinn für die School of Engineering, dass spezifische fachdidaktische Fragestellungen im Bereich der technischen Ausbildung in einem internationalen Netzwerk bearbeitet werden. Damit gelingen die gegenseitige Befruchtung von Forschung und Lehre und die Steigerung der Attraktivität unserer Schule für Studierende und Dozenten.

Referenzen

1. G. Tulodziecki, S. Grafe, B. Herzig: Gestaltungsorientierte Bildungsforschung und Didaktik: Theorie – Empirie – Praxis, Bad Heilbrunn, 2013.

2. L. H. Wong, C. K. Looi: What seams do we remove in mobile-assisted seamless ? A critical review of the literature. Computers & Education, 57 (4), 2364–2381, 2011.

3. L. H. Wong, M. Milrad, M. Specht: Seamless learning in the age of mobile connectivity, Springer, 2015.

4. A. Witzig, M. Prandini, A. Wolf, L. Kunath: Teaching Renewable Energy Systems by Use of Simulation Software: Experience at Universities of Applied Sciences, in In-Service Training, and from International Know-How Transfer, Eurosun 2016.

5. www.bodenseehochschule.org/ibh-labs/ibh-lab-seamless-learning

6. www.seamless-learning.eu

Appendix

A.1 Student Projects

O. ACAR, F. FEDDERSEN, *Prozessregelung einer Beschichtungsanlage für OLEDs*, Betreuer: K. Pernstich, O. Fluder (IMS), Semesterprojekt.

K. BAUR, P. KAELIN, *Aerodynamic analysis of an aerostat for Lighter Than Air (LTA) wind turbine applications, based on wind tunnel experiments*, Betreuer: G. Boiger, Y. Safa, Firmenpartner: ICP intern, Projektarbeit Aviatik.

A. BLEULER, N. SALIHI, J. STORSKOGEN, *Handgerät für die Messung von Schichtdicken im Baubereich*, Betreuer: N. Reinke, Bachelorarbeit Systemtechnik.

J. BRUDERER, A. RUPP, *Farbstoffsolarzellen: Weiterentwicklung der Software PECSIM*, Betreuer: M. Schmid, D. Bernhardsgrütter, Firmenpartner: G2E glass2energy SA, Villaz-St-Pierre, Projektarbeit Energie- und Umwelttechnik.

V. BUFF, L. PAGIONE, *Weiterentwicklung eines neuartigen Holzvergasers*, Betreuer: G. Boiger, T. Ott, C. Ritschard Firmenpartner: ICP intern, Projektarbeit Energie und Umwelttechnik.

M. CHRISTENSEN, P. STELLING, *Visualisierung in einem Smartgrid Planungstool*, Betreuer: A. Witzig, R. Knaak, Partner: Vela Solaris AG, Winterthur, Bachelorarbeit Informatik.

J. DUNST, *Fabrication and Characterization of Perovskite Solar Cells*, Betreuer: K. Pernstich, B. Ruhstaller, Vertiefungsarbeit Master of Science in Engineering.

S. EHRAT, C. WERDENBERG, *Ungleichverteilung in Anoden- und Kathodengasströmungen über SOFC-Stackhöhe detektieren und beheben*, Betreuer: T. Hocker, D. Meier, Firmenpartner: Hexis AG, Winterthur, Bachelorarbeit Energie und Umwelt.

N. EHRENBOLD, *Effizienzsteigerung und energetische Optimierung elektrostatischer Beschichtungsverfahren*, Betreuer: G. Boiger, N. Reinke, Firmenpartner: ICP intern, Bachelorarbeit Maschinentechnik.

A. HERZOG, S. KÜMIN, *Gekoppelte Simulation von dezentralen Energiesystemen und Gebäudeenergiebedarf*, Betreuer: A. Witzig, J. Borth, Firmenpartner: ICP intern, Bachelorarbeit Energie- und Umwelttechnik.

M. JANSEN, R. SCHELBERT, *Development and aerodynamic analysis of components for a Lighter Than Air (LTA) wind turbine, based on wind tunnel experiments*, Betreuer: G. Boiger, Y. Safa, Firmenpartner: ICP intern, Projektarbeit Aviatik.

D. MEIER, *Thermisch-fluidische Optimierung von Interkonnektoren von Brennstoffzellen vom Typ SOFC*, Betreuer: T. Hocker, C. Meier, Firmenpartner: Hexis AG, Winterthur, Vertiefungsarbeit Master of Science.

A. MEIER, R. ROPELATO, *Tieftemperatur-Messplatz mit Peltier-Elementen*, Betreuer: K. Pernstich, Semesterprojekt.

J. MEIER, G. SAUTER, *Entwicklung des Kraft-Wärmeverbundes eines neuartigen Holzvergasungsreaktors*, Betreuer: G. Boiger, A. Fassbind, Firmenpartner: Berchtold Apparatebau AG, Bachelorarbeit Energie und Umwelttechnik.

T. MESAREC, *Thermische Optimierung eines Lasttrennschalters*, Betreuer: T. Hocker, Firmenpartner: Woehner AG, Rödental (D), Vertiefungsarbeit Master of Science.

T. OTT, *Fortgeschrittene Simulations- und modellbasierte Weiterentwicklung eines porösen Diaphragmas zur pH-Wert Messung*, Betreuer: G. Boiger, M. Bonmarin, Firmenpartner: Dermolockin AG, Vertiefungsarbeit Masterstudiengang.

T. OTT, *Modellbasierte Weiterentwicklung eines porösen Diaphragmas zur pH-Wert Messung*, Betreuer: G. Boiger, Firmenpartner: Mettler Toledo AG, Vertiefungsarbeit Masterstudiengang.

D. SCHWYN, *Entwicklung eines neuartigen Holzvergasungsreaktors*, Betreuer: G. Boiger, A. Fassbind, Firmenpartner: Berchtold Apparatebau AG, Bachelorarbeit Maschinentechnik.

R. UHL, *Thermische Optimierung der Kristallisation von Schokolade – um Energie zu sparen und deren Qualität zu verbessern*, Betreuer: T. Hocker, Firmenpartner: Max Felchlin AG, Schwyz, Bachelorarbeit Energie- und Umwelttechnik.

M. VANKO, *Graphical User Interface for Electrical Model of Solar Cell for Hydrogen Production*, Supervisor: P. Cendula and S. Jurecka, SEMP Scholarship, BSc Thesis at the Faculty of Electrotechnical Engineering, University of Zilina, Slovakia.

P. VON SCHULTHESS, S. FAHRNI, *Bestimmung des Hautalters (Skinsure)*, Betreuer: N. Reinke, M. Bonmarin, Bachelorarbeit Systemtechnik.

S. WALKER, R. PETER, *Simulation of Solar Systems Compared to Measurements*, Supervisor: A. Witzig, Partner: M-H-University, Alicante, Spain, Bachelor's Degree Energy and Environmental Engineering.

A.2 Scientific Publications

S. ALTAZIN, S. ZÜFLE, E. KNAPP, C. KIRSCH, T.D. SCHMIDT, L. JÄGER, Y. NOGUCHI, W. BRÜTTING, B. RUHSTALLER, *Simulation of OLEDs with a polar electron transport layer*, Organic Electronics 39, 244–249, 2016.

S. ALTAZIN, S. ZÜFLE, E. KNAPP, C. KIRSCH, T. D. SCHMIDT, L. JÄGER, W. BRÜTTING, B. RUHSTALLER, *Combining Simulations and Experiments to Study the Impact of Polar OLED Materials*, SID Symposium Digest of Technical Papers, 47 (1), 1750–1753, 2016.

S. ALTAZIN, S. ZÜFLE, E. KNAPP, C. KIRSCH, L. JÄGER, T. D. SCHMIDT, W. BRÜTTING, B. RUHSTALLER, *On the role of polar molecules and the barrier for charge injection in OLEDs*, Proceedings of SPIE 9941, Organic Light Emitting Materials and Devices XX, 2016.

G. BOIGER, *Eulerian-LaGrangian model of particle laden flows and deposition effects in electrostatic fields based on OpenFoam*, International Journal of Multiphysics, 10 (2), 177–194, 2016.

G. BOIGER, *Characterization of particle laden flows and deposition behaviour in electro-static fields*, International Journal of Multiphysics, 10 (2), 195–204, 2016.

D. BURNAT, R. KONTIC, L. HOLZER, P. STEIGER, D. FERRI, A. HEEL, *Smart material concept: reversible microstructural self-regeneration for catalytic applications*, J. Mater. Chem. A., 4, 11939–11948, 2016.

O. CAGLAR, P. CARROY, P. A. LOSIO, I. SINICCO, *Nanocrystalline zinc oxide for surface morphology control in thin-film silicon solar cells*, Solar Energy Materials and Solar Cells, 144, 55–62, 2016.

L. CAPONE, P. MARMET, L. HOLZER, A. LAMIBRAC, J. DUJC, J. SCHUMACHER, A. LAMIBRAC, F. BÜCHI, J. BECKER, *An ensemble Monte Carlo simulation study of water distribution in porous gas diffusion layers for proton exchange membrane fuel cells*, Journal of Electrochemical Energy Conversion and Storage, submitted, 2016.

R. DELMELLE, R. DUARTE, T. FRANKEN, D. BURNAT, L. HOLZER, A. BORGSCHULTE, ET AL., *Development of improved nickel catalysts for sorption enhanced CO2 methanation*, Int. J. Hydrogen Energy, 41, 20185–20191, 2016.

J. DUJC, A. FORNER CUENCA, P. MARMET, M. COCHET, J. SCHUMACHER, P. BOILLAT, *Modelling the Effects of using Gas Diffusion Layers with Patterned Wettability for Advanced Water Management in Proton Exchange Membrane Fuel Cells*, Journal of Electrochemical Energy Conversion and Storage, submitted, 2016.

S. A. GEVORGYAN, N. ESPINOSA, L. CIAMMARUCHI, B. ROTH, F. LIVI, S. TSOPANIDIS, S. ZÜFLE, ET AL., *Baselines for Lifetime of Organic Solar Cells*, Advanced Energy Materials, 6, 1600910, 2016.

L. HOLZER, O. STENZEL, O. PECHO, T. OTT, G. BOIGER, M. GORBAR, ET AL., *Fundamental relationships between 3D pore topology, electrolyte conduction and flow properties: Towards knowledge-based design of ceramic diaphragms for sensor applications*, Materials & Design, 99, 314–327, 2016.

S. JENATSCH, L. WANG, M. BULLONI, A.C. VÉRON, B. RUHSTALLER, S. ALTAZIN, F. NÜESCH, R. HANY, *Doping Evolution and Junction Formation in Stacked Cyanine Dye Light-Emitting Electrochemical Cells*, ACS applied materials & interfaces, 8 (10), 6554–6562, 2016.

J. T. KIM, S. H. LEE, S. C. LEE, M. JAZBINSEK, K. MIYAMOTO, T. OMATSU, Y. S. LEE, O. P. KWON, *Terahertz Phonon Modes of Highly Efficient Electro-optic Phenyltriene OH1 Crystals*, The Journal of Physical Chemistry C, 120, 24360–24369, 2016.

J. Y. KIM, S. H. LEE, I. Y. CHOI, S. C. LEE, M. JAZBINSEK, W. S. KIM, S. K. KWAK, Y. S. HUH, J. W. KANG, O. P. KWON, *Stereoselective Inhibitors Based on Nonpolar Hydrocarbons for Polar Organic Crystals*, Crystal Growth & Design, 16, 6514–6521, 2016.

K. H. LEE, S. H. LEE, H. YUN, M. JAZBINSEK, J. W. KIM, F. ROTERMUND, O. P. KWON, *Multifunctional supramolecular building blocks with hydroxy piperidino groups: new opportunities for developing nonlinear optical ionic crystals*, CrystEngComm, 18, 5832–5841, 2016.

S. H. LEE, S. J. LEE, M. JAZBINSEK, B. J. KANG, F. ROTERMUND, O. P. KWON, *Electro-optic crystals grown in confined geometry with optimal crystal characteristics for THz photonic applications*, CrystEngComm, 18, 7311–7318, 2016.

S. H. LEE, G. H. LEE, K. H. LEE, M. JAZBINSEK, B. J. KANG, F. ROTERMUND, O. P. KWON, *In Situ Tailor-Made Additives for Molecular Crystals: A Simple Route to Morphological Crystal Engineering*, Crystal Growth & Design, 16, 3555–3561, 2016.

S. H. LEE, M. J. KOO, K. H. LEE, M. JAZBINSEK, B. J. KANG, F. ROTERMUND, O. P. KWON, *Quinolinium-based organic electro-optic crystals: Crystal characteristics in solvent mixtures and*

optical properties in the terahertz range, Materials Chemistry and Physics, 169, 62–70, 2016.

S. H. LEE, M. JAZBINSEK, C. P. HAURI, O. P. KWON, *Recent progress in acentric core structures for highly efficient nonlinear optical crystals and their supramolecular interactions and terahertz applications: Highlight*, CrystEngComm, 18, 7180–7203, 2016.

K. H. LE, A. KHARAGHANI, C. KIRSCH, E. TSOTSAS, *Pore Network Simulations of Heat and Mass Transfer inside an Unsaturated Capillary Porous Wick in the Dry-out Regime*, Transport in Porous Media, 114 (3), 623–648, 2016.

K. MANGIPUDI, V. RADISCH, L. HOLZER, C. A. VOLKERT, *A FIB-nanotomography method for accurate 3D reconstruction of open nanoporous structures*, Ultramicroscopy, 163, 38–47, 2016.

M. NEUMANN, J. STANEK, O. PECHO, L. HOLZER, V. BENES, V. SCHMIDT, *Stochastic 3D modeling of complex three-phase microstructures in SOFC-electrodes with completely connected phases*, Comput. Mater. Sci., 118, 353–364, 2016.

N. REINKE, *Reduktion des Pulverlackverbrauchs mit dem CoatMaster bei der Ernst Schweizer AG*, Besser lackieren, 2016.

O. STENZEL, M. NEUMANN, O. PECHO, V. SCHMIDT, L. HOLZER, *Predicting Effective Conductivities Based on Geometric Microstructure Characteristics*, AIChE Journal, 62 (5), 1834–1843, 2016.

A.3 Book Chapters

G. BOIGER,M. BOUWMAN, W. BRANDSTÄTTER, *Multiphase Simulations of a Lyocell Process*, Saarbrücken, Germany: LAP Lambert Academic Publishing, 2016.

A.4 Conferences and Workshops

S. ALTAZIN, S. ZÜFLE, E. KNAPP, C. KIRSCH, T. D. SCHMIDT, L. JÄGER, W. BRÜTTING, B. RUHSTALLER, *Combining Simulators and Experiments to Study the Impact of Polar OLED Materials*, SID Display Week, San Francisco USA, 2016.

S. ALTAZIN, L. STEPANOVA, K. LAPAGNA, J. WERNER, B. NIESEN, S. DE WOLF, C. BALLIF, B. RUHSTALLER, *Design of perovskite/crystalline silicon tandem solar cells*, Int. Conference on Hybrid and Organic Photovoltaics, Swansea UK, 2016.

S. ALTAZIN, L. STEPANOVA, K. LAPAGNA, P. LOSIO, J. WERNER, B. NIESEN, A. DABIRIAN, M. MORALES MASIS, S. DE WOLF, C. BALLIF, B. RUHSTALLER, *Design of Perovskite/Crystalline-Silicon Tandem Solar Cells*, 32nd European Photovoltaic Solar Energy Conference and Exhibition, Munich D, 2016.

G. BOIGER, T. OTT, L. HOLZER, D. PENNER, *Multi-parameter optimization method for the design of porous diaphragms applied in PH-measurement*, 11th International Conference of Multiphysics, Winterthur, 2016.

M. BOLDRINI, B. BONHOEFFER, M. JUHNKE, G. BOIGER, *Simulation of dispensing behavior of a micro valve in pharmaceutical applications*, 1st European COST Conference on Mathematics for Industry, Winterthur, 2016.

M. BOLDRINI, B. BONHOEFFER, M. JUHNKE, G. BOIGER, *Simulation of Non-Newtonian dispensing behaviour of a micro valve in pharmaceutical applications*, 11th International Conference of

Multiphysics, Winterthur, 2016.

D. BRUNNER, G. BOIGER, *Towards model based re-design of the copper electro-winning process*, 11th International Conference of Multiphysics, Winterthur, 2016.

D. BURNAT, R. KONTIC, L. HOLZER, A. MAI, A. HEEL, *SMART catalyst based on doped Sr-titanite for advanced SOFC anodes*, European Fuel Cell Forum, Lucerne, 2016.

L. CAPONE, P. MARMET, A. LAMIBRAC, J. DUJC, J. SCHUMACHER, *Ensemble-based study of equilibrium liquid water distribution in PEM gas diffusion layer* , MODVAL 13 Symposium for fuel cell and battery modeling and experimental validation, Lausanne, 2016.

P. CENDULA, *Modeling of charge transport and optical losses in metal oxide photoelectrodes*, Swiss PEC Symposium, Lausanne, 2016.

P. CENDULA, J. SCHUMACHER, *Spectroscopic modeling of photoelectrochemical water splitting*, COMSOL Conference, Munich D, 2016.

P. CENDULA, J. SCHUMACHER, *Spectroscopic modeling of photoelectrochemical water splitting*, 13th Symposium for Fuel Cell and Battery Modeling and Experimental Validation, Lausanne, 2016.

P. CENDULA, J. SCHUMACHER, *Simulation of photoelectrode impedance : extraction of water oxidation rate and recombination lifetime*, Solar Fuels Conference, Berlin D, 2016.

J. DUJC, A. FORNER CUENCA, M. COCHET, J. SCHUMACHER, P. BOILLAT, *Simulation-based optimization of patterned GDL for Water Management in PEFC*, MODVAL 13 Symposium for fuel cell and battery modeling and experimental validation, Lausanne, 2016.

J. DUJC, A. FORNER CUENCA, M. COCHET, J. SCHUMACHER, P. BOILLAT, *Numerical modeling of patterned porous materials for thermo-neutral fuel cells*, 3rd SCCER-Mobility Annual Conference, Zürich, 2016.

B. FURRER, N. ROSENBERGER, J. MUSIOLIK, T. HOCKER, *Workshop zur Marktreife von BZ-Heizgeräten*, Organisation: ZHAW, Teilnehmer: VSG, FOGA, Hexis AG, SOLIDpower GmbH, Buderus Heiztechnik AG, Vaillant Gruppe, Zürich, 2016.

M. GORBAR, Y. DE HAZAN, L. HOLZER, G. BOIGER, R. CERVERA, D. PENNER, *Controlled Porous Microstructure and its Effect on Transport Properties within YSZ Diaphragms of pH Electrodes*, 6th International Congress on Ceramics, German Ceramic Society and Fraunhofer Institute for Ceramic Technologies and Systems, Dresden D, 2016.

T. HOCKER, Y. SAFA, P. FAHRNI, D. MEIER, L. REJMAN, P. BRAUN, E. WINDHAB, *Controlled cooling and modeling the crystallization behavior of cocoa butter*, Choco Tec, Köln D, 2016.

L. HOLZER, O. PECHO, T. HOCKER, M. NEUMANN, V. SCHMIDT, *Optimization of Ni-YSZ Anode performance using virtual materials testing*, Modval 13. EPFL, Lausanne, 2016.

C. KIRSCH, S. ALTAZIN, R. HIESTAND, T. BEIERLEIN, M. CHRAPA, R. FERRINI, N. GLASER, J. GOLDOWSKY, A. MUSTACCIO, T. OFFERMANS, L. PENNINCK, B. RUHSTALLER, *Simulation of lateral charge transport in large-area optoelectronic semiconductor devices*, International Conference on the Simulation of Organic Electronics and Photovoltaics, Winterthur, 2016.

C. KIRSCH, S. ALTAZIN, R. HIESTAND, T. BEIERLEIN, R. FERRINI, T. OFFERMANS, L. PENNINCK, B. RUHSTALLER, *Electrothermal simulation of large-area semiconductor devices*, International Conference of Multiphysics, Zürich, 2016.

E. KNAPP, B. RUHSTALLER, *Origins of Negative Capacitance in Organic Single Layer Devices*, Int. Conference on the Simulation of Organic Electronics and Photovoltaics, Winterthur, 2016.

P. A. LOSIO, T. FEURER, S. BUECHELER, B. RUHSTALLER, *Evolutionary Optimization of TCO/Mesh Electrical Contacts in CIGS Solar Cells*, 32nd European Photovoltaic Solar Energy Conference and Exhibition, Munich D, 2016.

P. MARMET, J. DUJC, L. HOLZER, J. SCHUMACHER, A. LAMIBRAC, F. BÜCHI, *Multi-scale modeling of PEFCs*, 3rd SCCER-Mobility Annual Conference, Zürich, 2016.

M. NEUKOM, B. RUHSTALLER, *Preconditioned IV-curves: why does hysteresis of perovskite solar cells depend on the contact materials*, Int. Conference on Hybrid and Organic Photovoltaics, Swansea UK, 2016.

V. ORAVA, O. SOUCEK, P. CENDULA, *Multi-phase modelling of a reactive flow in fluidized bed reactors heated by internal tubes*, XXII International Conference on Chemical Reactors, London GB, 2016.

V. ORAVA, O. SOUCEK, P. CENDULA, *Multi-phase modelling of a reactive flow in fluidized bed reactors heated by internal tubes*, Multiphysics Conference 11, Winterthur, 2016.

V. ORAVA, O. SOUCEK, L. GUBLER, J. O. SCHUMACHER, P. CENDULA, *Multi-phase modeling of H2 generator coupled to a PEM FC*, 13th International Symposium on Modeling and Experimental Validation of Fuel cells and Batteries, Lausanne, 2016.

T. OTT, M. BONMARIN, G. BOIGER, *A thermo-, fluid-dynamic model of transient heat distribution within perfused human skin*, 11th International Conference of Multiphysics, Winterthur, 2016.

T. OTT, C. RITSCHARD, G. BOIGER, *Towards the model based development of a combined wood- and coal gasification reactor*, 11th International Conference of Multiphysics, Winterthur, 2016.

T. OTT, M. BONMARIN, G. BOIGER, *Active thermal imaging for skin cancer diagnostic supported by numerical 3D heat transfer skin model*, Yearly meeting of the Biomedical Photonics Network, Zürich, 2016.

N. REINKE, A. BARISKA, *Quality Improvement of Automotive Components by Real-Time Thickness Measurement*, Automotive Testing Expo, Stuttgart D, 2016.

B. RUHSTALLER, *Combining Simulations and Experiments to Study the Impact of Polar OLED Materials*, IMID Conference & Exhibition, South Korea, 2016.

B. RUHSTALLER, *Design, Characterization and Optimization of OLEDs for Lighting*, SwissPhotonics Solid-state Lighting Workshop, Muttenz, 2016.

Y. SAFA, T. HOCKER, *Developed Numerical Approach of The Melt-Crystals Phase-Changing Kinetics in Solidification Process*, The International Conference of Multiphysics, Winterthur, 2016.

J. SCHUMACHER, J. DUJC, P. MARMET, L. HOLZER, A. LAMIBRAC, A. FORNER-CUENCA, F. BÜCHI, *Influence of pore-scale material properties on the performance of proton exchange membrane fuel cells*, Material Challenges for Fuel Cell and Hydrogen Technologies ? From Innovation to Industry, Grenoble F, 2016.

L. STEPANOVA, S. ALTAZIN, B. RUHSTALLER, *Design of perovskite/crystalline silicon tandem solar cells*, Int. Conference on Simulation of Organic Electronics and Photovoltaics, Winterthur, 2016.

S. WEILENMANN, N. REINKE, G. BOIGER, *Multiphysics modelling of powder coating applications*, 11th International Conference of Multiphysics, Winterthur, 2016.

R. WIGOUTSCHNIGG, M. GUDER, S. WAGNER, L. MEIER, A. WITZIG, *Statik-Auslegung von aufgeständerten PV-Modulen mit Linearer Optimierung*, OTTI Symposium Photovoltaische Solarenergie, Bad Staffelstein D, 2016.

A. WITZIG, *Eigenmoden in optoelektronischen Resonatoren*, Rüdlinger-Tagung des Instituts für Angewandte Mathematik und Physik, Rüdlingen, 2016.

A. WITZIG, L. KUNATH, *Polysun Simulation Software in Teaching and Research at Various Academic Institutions in Switzerland*, Internationale Konferenz zur Simulation gebäudetechnischer Energiesysteme, 2016.

A. WITZIG, L. MEIER, S. WAGNER, *Integrale Planung mit 3D Dachplaner, Stückliste, Batteriespeicher, Power-to-Heat*, OTTI Symposium Photovoltaische Solarenergie, Bad Staffelstein D, 2016.

A. WITZIG, M. PRANDINI, A. WOLF, L. KUNATH, *Teaching Renewable Energy Systems by Use of Simulation Software: Experience at Universities of Applied Sciences, in In-Service Training and from International Know-How Transfer*, Eurosun, Mallorca S, 2016.

A. WITZIG, L. KUNATH, A. SOTNIKOV, J. KRIEG, *Kollektorerträge und Passivsolargewinne: Systemsimulation mit Mehrzonen-Gebäudesimulation*, OTTI Symposium Thermische Solarenergie, Bad Staffelstein D, 2016.

S. ZÜFLE, *Concentrated sunlight for accelerated testing of organic solar cells*, COST StableNextSol Meeting, Bratislava SK, 2016.

S. ZÜFLE, M. NEUKOM, S. ALTAZIN, B. RUHSTALLER, *Shedding Light on the Stability of Organic Solar Cells*, SimOEP, Winterthur, 2016.

S. ZÜFLE, B. RUHSTALLER, *Concentrated sunlight for accelerated aging of organic solar cells*, Int. Symposium on Organic Solar Cell Stability, Freiburg D, 2016.

A.5 Public Events

N. REINKE, A. BARISKA, *Winterthurer Oberflächentag 2016*, Winterthur, 2016.

B. RUHSTALLER, E. KNAPP, *Int. Conference on Simulation of Organic Electronics and Photovoltaics, SimOEP 2016*, Winterthur, 2016.

A. WITZIG, H. SOTNIKOVA, *Internationale Konferenz zur Simulation Gebäudetechnischer Energiesysteme*, Winterthur, 2016.

A.6 Patents

Y. SAFA, *Appareil pour la production d'énergie éolienne grâce aux courants d'air en haute altitude*, Patent pending, Bern, 2016.

A.7 Prizes and Awards

D. Brunner, Multiphysics Student Award at MULTIPHYSICS 2016, The International Society of Multiphysics, December, 2016.

Best poster prize for Vit Orava at the XXII International Conference on Chemical Reactors.

Winterthur Instruments received the Klimafond Award of Stadtwerk Winterthur.

A.8 Teaching

R. AXTHELM, *Mathematik: Analysis für Ingenieure 2 (EU und ET), FS16*, Bachelor of Science.

R. AXTHELM, *Mathematik: Numerik für Energie- und Umwelttechnik , HS16*, Bachelor of Science.

R. AXTHELM, *Mathematik für Ingenieure 3, HS16*, Bachelor of Science.

A. BARISKA, *Lineare Algebra für Ingenieure, FS16, HS16*, Bachelor of Science.

G. BOIGER, *Fluid- & Thermodynamik I für MT - Vorlesung & Praktikum FS16*, Bachelor of Science.

G. BOIGER, *Numerik für IT II – Vorlesung & Praktikum, FS16*, Bachelor of Science.

G. BOIGER, *Numerik für IT I – Vorlesung & Praktikum, HS16*, Bachelor of Science.

G. BOIGER, *Physik und Systemwissenschaften für AV II – Praktikum, FS16*, Bachelor of Science.

G. BOIGER, *Physik und Systemwissenschaften für AV I – Praktikum, HS16*, Bachelor of Science.

G. BOIGER, *Advanced Thermodynamics, HS16*, Master of Science in Engineering.

G. BOIGER, *Thermofluiddynamik Modellentwicklung mit OpenFoam I, HS16*, Master of Science in Engineering.

G. BOIGER, *Thermofluiddynamik Modellentwicklung mit OpenFoam II, HS16*, Master of Science in Engineering.

G. BOIGER, *Two Phase Flow with Heat and Mass Transfer, FS16*, Master of Science in Engineering.

A. HEEL, T. HOCKER, *Abgas- und Abwasserbehandlung, HS16*, Bachelor of Science.

T. HOCKER, *Fluid- und Thermodynamik 1 – Vorlesung, FS16*, Bachelor of Science.

T. HOCKER, *Fluid- und Thermodynamik 2 – Vorlesung, HS16*, Bachelor of Science.

T. HOCKER, *Systemphysik für Aviatik 1 – Praktikum, HS16*, Bachelor of Science.

T. HOCKER, *Systemphysik für Aviatik 2 – Praktikum, FS16*, Bachelor of Science.

M. JAZBINSEK, *Physik für Energie und Umwelttechnik 1 – Vorlesung & Praktikum*, Bachelor of Science.

M. JAZBINSEK, *Physik für Energie und Umwelttechnik 2 – Vorlesung & Praktikum*, Bachelor of Science.

C. KIRSCH, *Mathematik: Analysis für Ingenieure 4, FS16*, Bachelor of Science.

C. KIRSCH, *Mathematik: Lineare Algebra für Ingenieure 2, FS16*, Bachelor of Science.

C. KIRSCH, *Mathematik: Analysis für Ingenieure 1, HS16*, Bachelor of Science.

C. KIRSCH, *Mathematik: Numerische Methoden, HS16*, Bachelor of Science.

K. PERNSTICH, *Physik und Systemwissenschaft in Aviatik 1 – Praktikum*, Bachelor of Science.

K. PERNSTICH, *Physik und Systemwissenschaft in Aviatik 2 – Praktikum*, Bachelor of Science.

K. PERNSTICH, *Physik und Systemwissenschaften für Verkehrssysteme 1*, Bachelor of Science.

N. REINKE, *Physik für Informatiker, HS16*, Bachelor of Science.

R. RUHSTALLER, *Physik und Systemwissenschaften für Verkehrssysteme 1*, Bachelor of Science.

R. RUHSTALLER, *Applied Photonics*, Master of Science in Engineering.

G. SARTORIS, *4. Semester, CAE Kurs*, Masterstudiengang Micro- and Nanotechnology.

J. SCHUMACHER, *Analysis für Ingenieure 2 - FS16*, Bachelor of Science.

J. SCHUMACHER, *Analysis für Ingenieure 3 - HS16*, Bachelor of Science.

J. SCHUMACHER, *Organische Elektronik und Photovoltaik - FS16*, Bachelor of Science.

J. SCHUMACHER, *Multiphysics Modelling and Simulation FS16*, Master of Science in Engineering.

J. SCHUMACHER, *Numerical Simulation of Solar Cells FS16*, Master Online Photovoltaics.

M. SCHMID, *Mathematik: lineare Algebra für Ingenieure 1*, Bachelor of Science.

M. SCHMID, *Mathematik: lineare Algebra für Ingenieure 2*, Bachelor of Science.

M. SCHMID, *Math for Aviation: Linear Algebra 1*, Bachelor of Science.

A. WITZIG, *Physik: Felder und Wellen*, Bachelor Studiengang Elektrotechnik.

A. WITZIG, *Einführung in die Simulation von solarthermischen Anlagen*, Bachelor Studiengang Energie und Umwelttechnik.

A. WITZIG, *Einführung in die Simulation von solarthermischen Anlagen*, Bachelor Studiengang Energie und Umwelttechnik.

A.9 Spin-off Companies

NM Numerical Modelling GmbH
The engineering company, CH-Thalwil

www.nmtec.ch

Numerical Modelling GmbH works in the field of Computer Aided Engineering (CAE) and offers services and simulation tools for small and medium enterprises. Our core competence is knowledge transfer where we bridge the gap between scientific know-how and its application in the industry. With our knowledge from physics, chemistry and the engineering sciences we are able to support your product development cycle and to conform to yours time and budget constraints. We often create so-called customer specific CAE tools in which the scientific knowledge required for your product is embedded. In this form, it is easily deployed within your R&D department and supports actual projects as well as improving the skills of your staff. Ask for our individual consulting service which covers all areas of scientific knowledge transfer without obligation.

FLUXiM

www.fluxim.com

Fluxim is a provider of device simulation software and measurement hardware to the display, lighting and photovoltaics community worldwide. Our principal activity is the development and the marketing of the simulation software SETFOS and LAOSS, as well as the all-in-one characterization platform PAIOS. SETFOS was designed to simulate light propagation and charge transport in large-area opto-electronic devices such as organic light-emitting diodes (OLEDs) and solar cells while PAIOS measures the dynamic opto-electrical response in time and frequency domain which supports the determination of material parameters. Our R&D tools are used worldwide in industrial and academic research labs for the development of devices and semiconducting materials with improved performance as well as the study of device physics.

WinterthurInstruments
noncontact and nondestructive testing of coatings

www.winterthurinstruments.ch

Winterthur Instruments AG develops measurement systems for fast non-contact and non-destructive testing of industrial coatings. These measurement systems can be used to determine coating thicknesses, material parameters, e. g. porosity and contact quality, e. g. to detect delamination. The system is based on optical-thermal measurements and works with all types of coating and substrate materials. Our measurement systems provide the unique opportunity of non-contact and non-destructive testing of arbitrary coatings on substrates.

DERMOLOCKIN

www.dermolockin.com

Dermolockin GmbH is a recently founded spin-off company developing active thermography-based setups for dermatological applications. The main focus lies in the detection and characterization of cutaneous cancerous lesions with lock-in thermal imaging methods.

A.10 ICP-Team

Name	Function	e-Mail
Andor Bariska	Lecturer	bara@zhaw.ch
Dr. Tilman Beierlein	Research Associate	beir@zhaw.ch
David Bernhardsgrütter	Research Associate	bens@zhaw.ch
Dr. Gernot Boiger	Lecturer	boig@zhaw.ch
Marlon Boldrini	Research Assistant	bolm@zhaw.ch
Dr. Mathias Bonmarin	Lecturer	bmat@zhaw.ch
Daniel Brunner	Research Assistant	brni@zhaw.ch
Dr. Peter Cendula	Research Associate	cend@zhaw.ch
Teresa D'Onghia	Administrative Assistant	dong@zhaw.ch
Matthias Diethelm	Research Assistant	diei@zhaw.ch
Jonas Dunst	Research Assistant	duns@zhaw.ch
Daniel Fehr	Research Assistant	fehd@zhaw.ch
Samuel Hauri	Research Associate	haui@zhaw.ch
Prof. Dr. Thomas Hocker	Lecturer	hoto@zhaw.ch
Dr. Lorenz Holzer	Research Associate	holz@zhaw.ch
Dr. Mojca Jazbinsek	Lecturer	jazb@zhaw.ch
Dr. Lukas Keller	Research Associate	kelu@zhaw.ch
Dr. Christoph Kirsch	Research Associate	kirs@zhaw.ch
Dr. Evelyne Knapp	Research Associate	hube@zhaw.ch
Dr. Marcin Krajewski	Research Associate	kraj@zhaw.ch
Daniel Meier	Research Assistant	meda@zhaw.ch
Martin Neukom	Research Assistant	neko@zhaw.ch
Tobias Ott	Research Assistant	otto@zhaw.ch
Dr. Kurt Pernstich	Lecturer	pern@zhaw.ch
Dr. Uros Puc	Research Associate	pucu@zhaw.ch
Markus Regnat	Research Assistant	rega@zhaw.ch
Prof. Dr. Nils Reinke	Lecturer	rein@zhaw.ch
Claude Ritschard	Research Assistant	ritc@zhaw.ch
Prof. Dr. Beat Ruhstaller	Lecturer	ruhb@zhaw.ch
Dr. Yasser Safa	Research Associate	safa@zhaw.ch
Dr. Guido Sartoris	Research Associate	srts@zhaw.ch
Hanna Sotnikova	Research Assistant	sotn@zhaw.ch
Andreas Schiller	Research Assistant	scdr@zhaw.ch
Dr. Matthias Schmid	Lecturer	scmi@zhaw.ch
Prof. Dr. Jürgen Schumacher	Lecturer	schm@zhaw.ch
Moreno Torroni	Research Assistant	toro@zhaw.ch
Dr. Roman Vetter	Research Associate	vetr@zhaw.ch
Urs Vögeli	Research Assistant	voee@zhaw.ch
Stephan Weilenmann	Research Assistant	weit@zhaw.ch
Dr. Andreas Witzig	Lecturer, Head ICP	wita@zhaw.ch
Simon Züfle	Research Assistant	zufe@zhaw.ch

A.11 Location

ICP Institute of Computational Physics

Technikumstrasse 9
P.O. Box
CH-8401 Winterthur

www.icp.zhaw.ch

Contact

Andreas Witzig
Phone +41 58 934 45 73
andreas.witzig@zhaw.ch

Administration

Esther Spiess
Phone +41 58 934 73 38
esther.spiess@zhaw.ch

Teresa D'Onghia
Phone +41 58 934 67 62
teresa.donghia@zhaw.ch

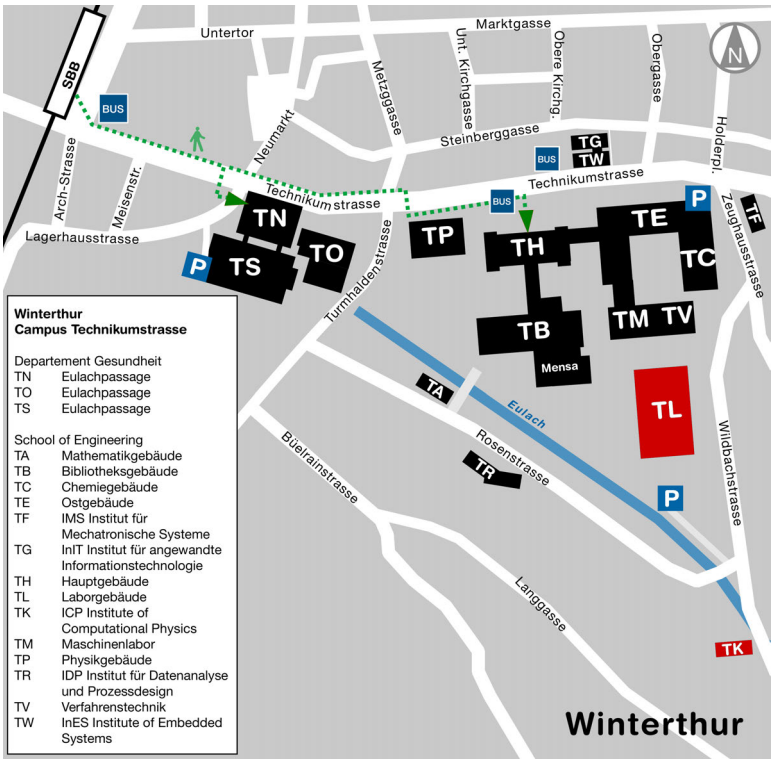

TK building

TL building

Zurich University
of Applied Sciences

School of Engineering

ICP Institute of
Computational Physics

Technikumstrasse 9
P.O. Box
CH-8401 Winterthur

Phone +41 58 934 71 71
info.engineering@zhaw.ch
www.zhaw.ch/icp